ISSN 2096-7071
CN 10-1629/R1

CHINA CDC WEEKLY

Vol. 2 No. 23 Jun. 5, 2020

CCDC weekly

中国疾病预防控制中心周报

ISSN 2096-7071

China CDC Weekly

Cover Image: The poster for the 49th World Environment Day, designed by Chao Wang, National Institute of Environmental Health, China CDC.

Announcements

The 49th World Environment Day — June 5, 2020

Xiaoming Shi[1,#]; Tiantian Li[1]

World Environment Day, established by the United Nations (UN) at the first Conference on the Human Environment in 1972, is designated each year on June 5 to forge a basic common outlook on how to address the challenge of preserving and enhancing the human environment. World Environment Day is one of the principal vehicles through which the UN stimulates worldwide awareness of the environment and enhances political attention and action, and it is now the most renowned day for environmental action with more than 100 countries joining.

The Ministry of Ecology and Environment announced the theme for the 2020 World Environment Day — "Act towards a Beautiful China", intending to encourage all citizens of the general public to actively contribute to the building of a civilization focused on ecological protection through working together to prevent and control pollution and to develop a beautiful country with blue skies, green lands, and clean waters (*1*).

In the last several decades, environmental pollution has become increasingly prominent in China with several key aspects such as the atmosphere (urban pollution, greenhouse gases, etc.), land (desertification, chemical pollution, etc.), water (pollution including antibiotics/nanopollutants, etc.), oceans (plastic waste, polar melting, etc.), and biodiversity (extinction of genes, species, and ecosystems, etc.). The environmental factors related to health impact have become a significant public health concern in China (*2*). Revised environmental protection law (2015), Healthy China 2030 etc. address the importance of enhancing environmental monitoring, health surveillance, and risk assessment system in the environmental health activities. These policies also stress the importance of carrying out work on environmental health for protecting public health.

In this issue, we invited colleagues from National Institute of Environmental Health, China CDC, Chinese Research Academy of Environmental Sciences, and Fudan University to report their latest research findings on environmental health. Liu et al. assessed the air quality after the implementation of the Clean Air Action in Beijing-Tianjin-Hebei, China. They found significant improvements in air quality and also explored the evolution of air pollution characteristics. Zhong et al. reported the association between high temperature and non-accidental and circulatory mortality in 130 Chinese counties from 2013 to 2018 and found that the daily mean temperature was the optimal indicator for high temperature related mortality risk assessment. Lyu et al. investigated the antibiotics in drinking water and reported the health risks in 6 large river basins, inland river areas, and key lake and reservoir areas of China in 2017, which revealed the potential antibiotic threats for public health in China. Fan et al. conducted a baseline investigation on residential $PM_{2.5}$ pollution in 12 cities in China in 2018 and suggested the necessity for controlling the residential $PM_{2.5}$ pollution in China. Niu et al. found the positive association between short-term exposure to ambient ozone and outpatient visits for respiratory diseases in 5 cities in China, which may further guide policy-making for reducing ozone air pollution and improving public health. We hope these studies in this special issue may encourage readers to better understand environmental and health issues and provide public health policy implications for future environmental health policy-making in China.

doi: 10.46234/ccdcw2020.104

Corresponding author: Xiaoming Shi, shixm@chinacdc.cn.

1 China CDC Key Laboratory of Environment and Population Health, National Institute of Environmental Health, Chinese Center for Disease Control and Prevention.

Submitted: May 24, 2020; Accepted: May 25, 2020

REFERENCES

1. Ministry of Ecology and Environment of the People's Republic of China. Ministry of ecological and environment issued the theme poster of environment day during the 6th five year of 2020. http://www.mee.gov.cn/ywgz/xcjy/xccpzyk/hb/202005/t20200522_780328.shtml. [2020-05-24]. (in Chinese).
2. United Nations Environment Program. Global Environment Outlook 6, 2019. https://www.unenvironment.org/resources/global-environment-outlook-6. [2020-05-24].(in Chinese).

Preplanned Studies

High Temperature and Risk of Cause-Specific Mortality in China, 2013−2018

Yu Zhong[1]; Chen Chen[1]; Qing Wang[1]; Tiantian Li[1,#]

Summary

What is already known about this topic?

High temperature is a well-recognized public health threat and may increase mortality risks, especially mortality risks involving diseases of the circulatory system.

What is added by this report?

Using a six-year time series analysis, the differences of daily mean, maximum, minimum temperature were explored in assessing the health effects of high temperatures in nationwide and at climatic-zone level, and population groups susceptible to high temperatures were identified.

What are the implications for public health practice?

This study suggests that the daily mean temperature is the optimal indicator for high temperature exposure in heat-related health risk assessments and early warnings. The policy measures of heat-related public health protection should be made considering regional distribution, sensitive diseases, and vulnerable populations.

There is no nationally representative conclusion on associations between high temperature and cause-specific mortality, and it is unclear which indicator is applicable for evaluating health risks for high temperature. This study intends to estimate associations between high temperature and cause-specific mortality and to identify suitable indicators for heat-related risk assessment. We applied a time-series study with generalized linear model in 130 Chinese counties to estimate the national and climatic-zone associations between 3 high temperature indicators and cause-specific mortality for summer months of 2013–2018. We also considered estimation for sex and age groups. We found that all 3 high temperature indicators had positive associations with cause-specific mortality, and associations between daily mean temperature and cause-specific mortality were relatively higher than daily maximum and minimum temperature. Female and the elderly aged 75 years old or more were the population groups more susceptible to heat-related mortality. This study provides key information for future heat-related health risk assessments and early warning systems and suggests that public health action plans on high temperatures should be tailored to vulnerable population and climatic zones.

The influence of high temperature on human health has been a worldwide major public concern during the past few decades (*1*–*4*). During the 2003 heat wave in France, the number of deaths related to high temperature was 3,306, including 3,004 deaths from heat-related circulatory system diseases (*5*). Many studies have found that the mortality rates of ischemic heart disease (IHD) and cerebrovascular disease were associated with high temperature (*4*). The Intergovernmental Panel on Climate Change (IPCC) has predicted that global temperature is likely to increase 1.5 ℃ between the 2030s and 2050s, and global extreme heat events will increase in frequency, duration, and intensity (*6*). Previous studies have predicted that heat-related mortality may increase by 66%, 257%, and 535% by the 2020s, 2050s, and 2080s, respectively (*7*). Along with rising temperature levels under climate change, the effects of high temperature on human health will likely become more serious in the future.

However, as the association between high temperature and mortality may vary by study area, there is no consistent conclusion on the quantitative effect of high-temperature to mortality (*8*). Furthermore, there is currently no agreement on which indicator should be used for high temperature measurements to evaluate health risks (*8*–*9*). Under the conditions of different climatic zones, it is especially necessary to identify the appropriate indicator to conduct the high temperature related health risk assessment and establish the early warning system in China.

The main purpose of this study is to evaluate the effect of high temperature indicators (daily mean, maximum, and minimum temperature) on mortality and determine the optimal high temperature indicator. Moreover, this study also sought to estimate the mortality effects of high temperature on different population groups and different climatic zones.

We linked three indicators (mean, maximum, and minimum) on daily temperature with daily mortality counts for the summer months (June, July, August, and September) of 2013 to 2018 in 130 Chinese counties. A map of climatic zones was provided by the China Meteorological Administration (*10*) (Supplementary Figure S1 available in http://weekly.chinacdc.cn/). These 130 counties were distributed in different climatic zones with 42 counties in subtropics, 71 counties in warm temperature zone, 15 counties in middle temperate zone, and 2 counties in plateau climatic zone.

Meteorological data were collected from the European Centre for Medium-Range Weather Forecasts. The daily mortality data were obtained from the Disease Surveillance Point System (DSPS) of China CDC. Based on this dataset, the daily counts of non-accidental mortality and circulatory system disease mortality were calculated. The causes of circulatory system mortality, including cerebrovascular disease, ischemic heart disease, myocardial infarction, and stroke, were also analyzed in this study. The International Statistical Classification of Disease Version 10 (ICD-10) of the included diseases was provided in supplementary material (available in http://weekly.chinacdc.cn/). We classified the deaths by age (0–64, 65–74, and ≥75) and sex (female and male). To adjust for the confounding effects of air pollutants, we collected air pollution data, including the concentrations of fine particulate matter ($PM_{2.5}$) and ozone (O_3), and the data sources and cleaning principles of air pollutants had been described in previous study (*11*) .

The associations between high temperature and mortality were investigated in a two-stage analysis. First, we analyzed associations of high temperature and cause-specific mortality in each county by using a generalized liner model (GLM) with quasi-Poisson regression. Second, we pooled estimates nationwide and at climatic-zone scales by a random effects meta-analysis. Considering the lagged effect of high temperature, the moving average exposure of previous 1 day and current day (lag 01) was the largest and used in the core model to assess heat effects (Supplementary Figure S2 available in http://weekly.chinacdc.cn/). We also examined the effects at other lags of high temperature. Furthermore, in order to identify vulnerable populations for heat-related mortality, we performed the subgroup analysis by sex (female and male) and age (0–64, 65–74, and ≥75) groups. We conducted sensitivity analysis to validate the robustness of the core model. The temperature-mortality association was estimated by percent increase in mortality risk and its 95% confidence interval (CI) with 1 ℃ increase of daily high temperature indicators. Detailed information on the statistical model and sensitivity analysis were available in the supplementary materials. All analyses were performed by R statistical software (version 4.0.0; The R Foundation for Statistical Computing).

During the study period, the 24-hour average value of daily mean, maximum, and minimum temperature of all the studying counties was 24 ℃, 29 ℃, and 20 ℃, respectively; the daily mean deaths of non-accidental were 9 ± 6 and circulatory system disease were 4 ± 3 per day (Table 1). For each climatic zone, the descriptive results were shown in supplementary Table S1 (available in http://weekly.chinacdc.cn/).

At the national level, daily mean, maximum temperature, and minimum temperature were all significantly associated with the six causes of mortality. Using Z test, we found that associations between daily mean temperature and the 6 causes of mortality were more significant (Figure 1 and Supplementary Table S2 available in http://weekly.chinacdc.cn/). The 1 ℃ increase of daily mean temperature was estimated to have a 2.71% (95% CI: 2.25%–3.19%) increase of heat effect on IHD mortality, while the heat effect on stroke mortality showed a lower level increase (1.67% with 95% CI: 1.28%–2.07%).

For the climatic zones, the associations between daily mean temperature and the six causes of mortality in all climate zones were consistent with nationwide results, especially in warm temperature zones with 1 ℃ increase in daily mean temperature, the mortality risk for IHD was estimated to increase by 2.95%, (95% CI: 2.31%–3.60%), and the stroke has the lowest mortality risk increase 1.52%, (95% CI: 0.99%–2.05%) (Figure 1).

For subgroup analysis, females and people older than 75 years were more vulnerable to high temperatures. For females, mortality risk of circulatory system disease was estimated to increase by 3.12% (95% CI: 2.67%–3.57%). For the group aged over 75 years old, the mortality risk of circulatory system disease was estimated to increase by 3.00% (95% CI: 2.59%–3.42%) (Table 2).

TABLE 1. Summary statistics of mortality, meteorology, and air pollution of summer months in 2013 to 2018 nationwide

Variable	Mean ± SD	Median (P_{25}, P_{75})
Cause of mortality		
Non-accidental mortality	9 ± 6	7 (4, 12)
Circulatory system disease	4 ± 3	3 (2, 6)
Cerebrovascular disease	2 ± 2	1 (0, 3)
Ischemic heart disease	2 ± 2	1 (0, 3)
Myocardial infarction	1 ± 1	1 (0, 1)
Stroke	1 ± 2	1 (0, 2)
Meteorology		
Temperature (℃)		
Daily mean temperature	24 ± 5	25 (21, 27)
Daily maximum temperature	29 ± 5	29 (26, 32)
Daily minimum temperature	20 ± 5	21 (17, 24)
Relative humidity (%)		
Daily mean relative humidity	72 ± 16	75 (63, 83)
Air pollution		
$PM_{2.5}$ concentration (24-hour average, μg/m^3)	39 ± 28	32 (20, 50)
O_3 concentration (24-hour average, μg/m^3)	73 ± 35	70 (48, 95)

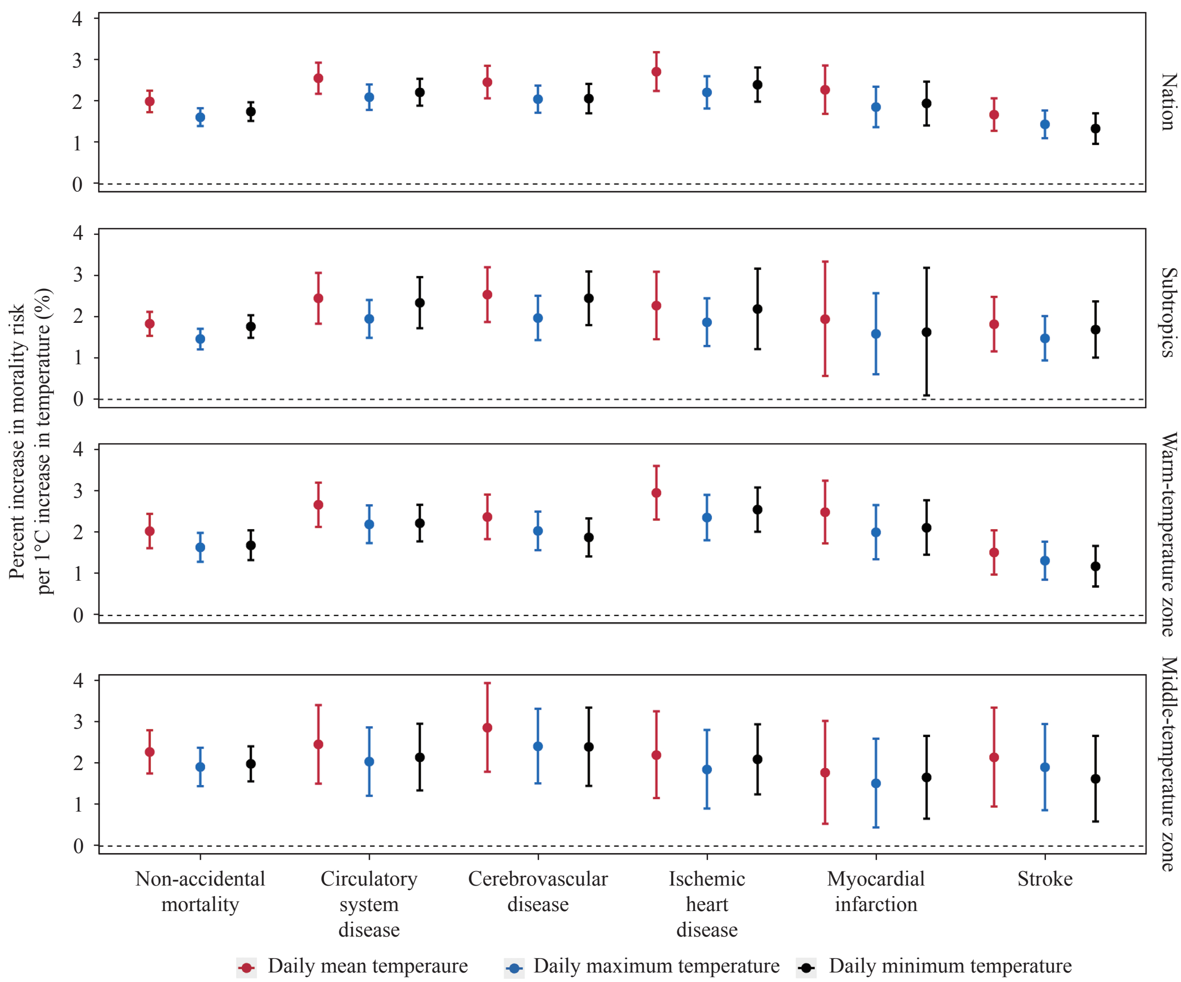

FIGURE 1. Percent increase in mortality risk due to high temperature during summer months of 2013 to 2018 in nation and climate zones.

TABLE 2. Subgroups estimates of high temperature and mortality risk for the summer months in 2013 to 2018 nationwide.

Cause of death	Exposure	Percent increase in mortality risk (%)(95%CI)				
		Female	Male	Age 0–64	Age 65–74	Age ≥75
Non-accidental mortality	Daily mean temperature	2.54 (2.20–2.88)	1.62 (1.39–1.85)	1.06 (0.77–1.34)	1.82 (1.50–2.15)	2.53 (2.21–2.85)
	Daily maximum temperature	2.05 (1.77–2.33)	1.30 (1.10–1.50)	0.86 (0.62–1.10)	1.46 (1.19–1.73)	2.04 (1.78–2.31)
	Daily minimum temperature	2.24 (1.94–2.54)	1.42 (1.22–1.62)	0.90 (0.63–1.17)	1.54 (1.26–1.83)	2.26 (1.97–2.56)
Circulatory system diseases	Daily mean temperature	3.12 (2.67–3.57)	2.08 (1.71–2.46)	1.16 (0.66–1.65)	2.51 (2.06–2.96)	3.00 (2.59, 3.42)
	Daily maximum temperature	2.57 (2.19–2.94)	1.70 (1.38–2.01)	0.94 (0.52–1.37)	2.03 (1.64–2.43)	2.47 (2.13–2.80)
	Daily minimum temperature	2.72 (2.32–3.12)	1.80 (1.46–2.13)	1.00 (0.58–1.42)	2.08 (1.67–2.48)	2.65 (2.26–3.03)

DISCUSSION

In this study, we assessed associations between high temperature indicators and six causes of mortality. We found that high temperature indicators had positive associations with six causes of mortality, and the daily mean temperature was estimated to have higher mortality-effect than daily maximum and minimum temperature. The elderly group (aged 75 years old or more) and female were more vulnerable to heat-related mortality risks.

A study in US showed that a 5 ℃ increase in mean, maximum, and minimum temperature was accompanied by a non-accidental mortality increase of 3.58%, 2.27%, and 3.14%, respectively (*1*). The association between mean temperature and non-accidental mortality was higher than that of the maximum and minimum temperature (*1*), which was consistent with our study. However, a study of nine counties in California found that the daily minimum temperature had a higher association with mortality than daily mean and maximum temperature (*2*). The inconsistency may be due to the differences in geographical characteristics and demographic structure (*8*), as well as the difference in the sensitivity of the population to night temperature changes (*2*). In many countries, daily mean temperature was widely used as the exposure indicator for high temperature monitoring and health risk assessments (*9*). The daily mean temperature represents the average level of exposure and had a good representativeness when applied to estimating health risks due to high temperature. This suggested that we could give priority to daily mean temperature as the exposure measurement indicator when conducting heat-health early warning research.

Previous studies had found that high temperature was associated with deaths due to circulatory system disease (*4*). A worldwide meta-analysis reported that high temperature increased 1 ℃, the mortality risks of circulatory increased by 1.3% (95% CI: 1.1%–1.5%) (*4*), which was consistent with our findings at the national-level and climatic-zone level.

Some previous studies had not found any differences of high-temperature-related mortality risk between genders (*3*). Through subgroup analysis, we observed that females were a high-risk group for high temperature and that the elderly aged over 75 years old were more vulnerable to high temperature. The elderly may be more likely to be in poorer physical health than those in younger groups and may more likely to have basic diseases. In addition, the elderly had a more limited ability to perceive changes in the temperature of the external environment, so their adaptability to high temperatures was reduced (*3*).

This study was subject to at least one limitation. In addition to the single temperature indicator, some studies have constructed composite indicators that included both temperature and humidity variables (*8*–*9*). Since this model controlled the confounding effects of humidity factors, in order to avoid the variable collinearity, the health impact of the composite indicator had not been estimated in this study and therefore further analysis is needed.

Fundings: This study was funded by the Special Foundation of Basic Science and Technology Resources Survey of Ministry of Science and Technology of China (Grant No. 2017FY101204), the Young Scholar Scientific Research Foundation of National Institute of Environmental Health, China CDC (No. 2020YSRF_02) and the National Key Research and Development Program of China (2017YFC0211706).

doi: 10.46234/ccdcw2020.105

Corresponding author: Tiantian Li, litiantian@nieh.chinacdc.cn.

[1] China CDC Key Laboratory of Environment and Population Health, National Institute of Environmental Health, Chinese Center for Disease Control and Prevention, Beijing, China.

Submitted: May 19, 2020; Accepted: May 24, 2020

REFERENCES

1. Zanobetti A, Schwartz J. Temperature and mortality in nine US cities. Epidemiology 2008;19(4):563 – 70. http://dx.doi.org/10.1097/EDE.0b013e31816d652d.
2. Basu R, Feng WY, Ostro BD. Characterizing temperature and mortality in nine California counties. Epidemiology 2008;19(1):138 – 45. http://dx.doi.org/10.1097/EDE.0b013e31815c1da7.
3. Huang ZJ, Lin HL, Liu YN, Zhou MG, Liu T, Xiao JP, et al. Individual-level and community-level effect modifiers of the temperature-mortality relationship in 66 Chinese communities. BMJ Open 2015;5(9):e009172. http://dx.doi.org/10.1136/bmjopen-2015-009172.
4. Moghadamnia MT, Ardalan A, Mesdaghinia A, Keshtkar A, Naddafi K, Yekaninejad M S. Ambient temperature and cardiovascular mortality: a systematic review and meta-analysis. PeerJ 2017;5(8):e3574. http://dx.doi.org/10.7717/peerj.3574.
5. Fouillet A, Rey G, Laurent F, Pavillon G, Bellec S, Guihenneuc-Jouyaux C, et al. Excess mortality related to the August 2003 heat wave in France. Int Arch Occup Environ Health 2006;80(1):16 – 24. http://dx.doi.org/10.1007/s00420-006-0089-4.
6. IPCC. Global warming of 1.5 °C. 2018. https://www.ipcc.ch/site/assets/uploads/sites/2/2019/06/SR15_Full_Report_Low_Res.pdf. [2020-05-18]
7. Vardoulakis S, Dear K, Hajat S, Heaviside C, Eggen B, McMichael A J. Comparative assessment of the effects of climate change on heat-and cold-related mortality in the united kingdom and Australia. Environ Health Perspect, 2014;122(12):1261 – 92. http://dx.doi.org/10.1289/ehp.1307524.
8. Lin YK, Chang CK, Li MH, Wu YC, Wang YC. High-temperature indices associated with mortality and outpatient visits: characterizing the association with elevated temperature. Sci Total Environ 2012;427-428:41 – 9. http://dx.doi.org/10.1016/j.scitotenv.2012.04.039.
9. Casanueva A, Burgstall A, Kotlarski S, Messeri A, Morabito M, Flouris AD, et al. Overview of existing heat-health warning systems in Europe. Int J Environ Res Public Health 2019;16(15):2657. http://dx.doi.org/10.3390/ijerph16152657.
10. China Meteorological Administration. Climatological atlas of the people's republic of China. Beijing: China Cartographic Publishing House, 1979. (In Chinese).
11. Chen C, Li TT, Wang LJ, Qi JL, Shi WY, He MZ, et al. Short-term exposure to fine particles and risk of cause-specific Mortality—China, 2013–2018. China CDC Weekly 2019;1(1):8 – 12. doi:10.46234/ccdcw2019.004.

Supplementary Material

Mortality data

This study includes six causes of mortalities: Non-accidental mortality (ICD-10:A00-R99), Circulatory system disease (ICD-10:I00-I99), Cerebrovascular disease (ICD-10:I60-I69), Ischemic Heart Disease (ICD-10:I20-I25), Myocardial infarction (ICD-10:I21-I23), and Stroke (ICD-10:I60-I64). They are classified by the International Statistical Classification of 10th Revision (ICD-10; World Health Organization 2007).

Meteorological data

Temperature and dewpoint temperature during summer of 2013 to 2018 in 130 counties were collected from the European Centre for Medium-Range Weather Forecasts (https://cds.climate.copernicus.eu/cdsapp#!/dataset/reanalysis-era5-land?tab=form). First, we calculated the daily temperature and dewpoint temperature in each county by using R software (version 4.0.0; The R Foundation for Statistical Computing); then, according to the equation, we calculated daily relative humidity by temperature and dewpoint temperature for each county.

$$e = 6.11 * 10^{\left(\frac{7.5*T_d}{237.3+T_d}\right)}$$

$$e_s = 6.11 * 10^{\left(\frac{7.5*T}{237.3+T}\right)}$$

$$rh = \frac{e}{e_s} * 100$$

In the formula, T was temperature (℃), T_d was dewpoint temperature (℃), e was the actual vapor pressure, e_s was saturated vapor pressure, rh was the relative humidity (%).

Statistical model

$$LogE(Y_t) = Intercep_t + \beta_1 Var_t + \beta_2 RHmean_t + ns(time, df) + dow$$

In the formula, t was the day of observation; Y_t was the observed daily death counts on day t; β_1 was the regression coefficient of Var_t; β_2 represented regression coefficient of daily mean relatively humidity; Var_t was the observed variable of daily mean temperature, daily maximum temperature, daily minimum temperature on day t; $RHmean_t$ represented mean relative humidity at day t; ns ($time$, df) represented the natural-spline function of time trend and was used a natural cubic regression spline with 3 degrees of freedom (df) in summer of per year to control the long-term and seasonal trends; dow was a dummy variable to control the week effect.

Lagged effect of high temperature

In this study, we studied the lag structures for high temperature and cause-specific mortality. The association between the current day (lag0) of high temperature and cause-specific mortality was tested. What is more, the moving average lag of 1 day to the moving average lag of 7 days of high temperature were also examined in this study. The mortality effect of moving average exposure of previous 1 day and current day (lag 01) was highest among all the lagged exposures (Supplementary Figure S2).

Z test

To determine if the risk estimates of high temperature indicators were statistically different, we used the daily mean temperature as a reference and compared it with the daily maximum and minimum temperature respectively (Supplementary Table S2).

$$z = \frac{\beta_1 - \beta_2}{\sqrt{se_1(\beta_1)^2 + se_2(\beta_2)^2}}$$

The formula z value was the Z test score for pairwise comparison; the β_1 was the regression coefficient of the daily mean temperature; β_2 was the regression coefficient of the daily maximum temperature or daily minimum temperature; se_1 represented the standard error of daily mean temperature; se_2 represented the standard error of daily maximum temperature or daily minimum temperature.

Sensitivity analysis

Table S3 showed the sensitivity analysis results of daily mean temperature and non-accidental mortality: first, specification of degrees of freedom in the smooth functions of time (df_{time}=2, 4) to observe whether the effect estimation changed; second, inclusion of $PM_{2.5}$ and O_3 as potential confounders on the relationship between high temperature and health, respectively. Sensitivity analysis showed that the core model was robust (Table S3).

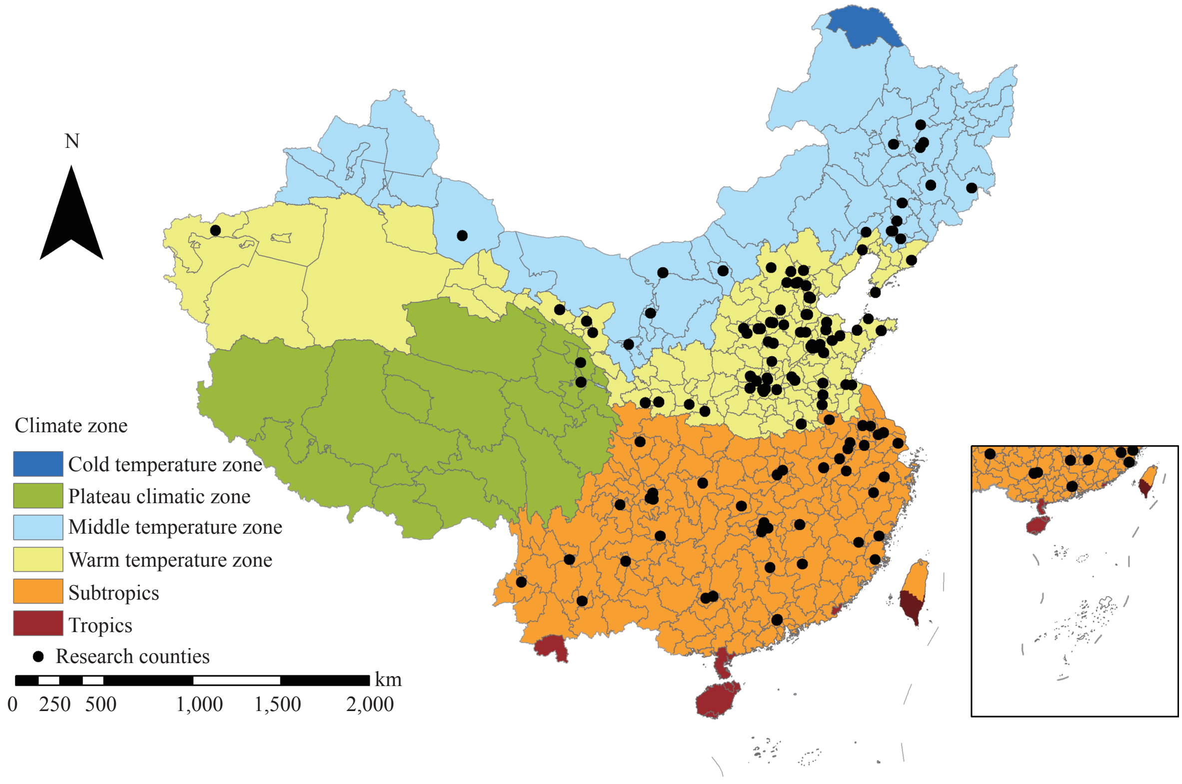

SUPPLEMENTARY FIGURE S1. The map of climatic-zones and the distribution of the surveyed 130 counties in China.

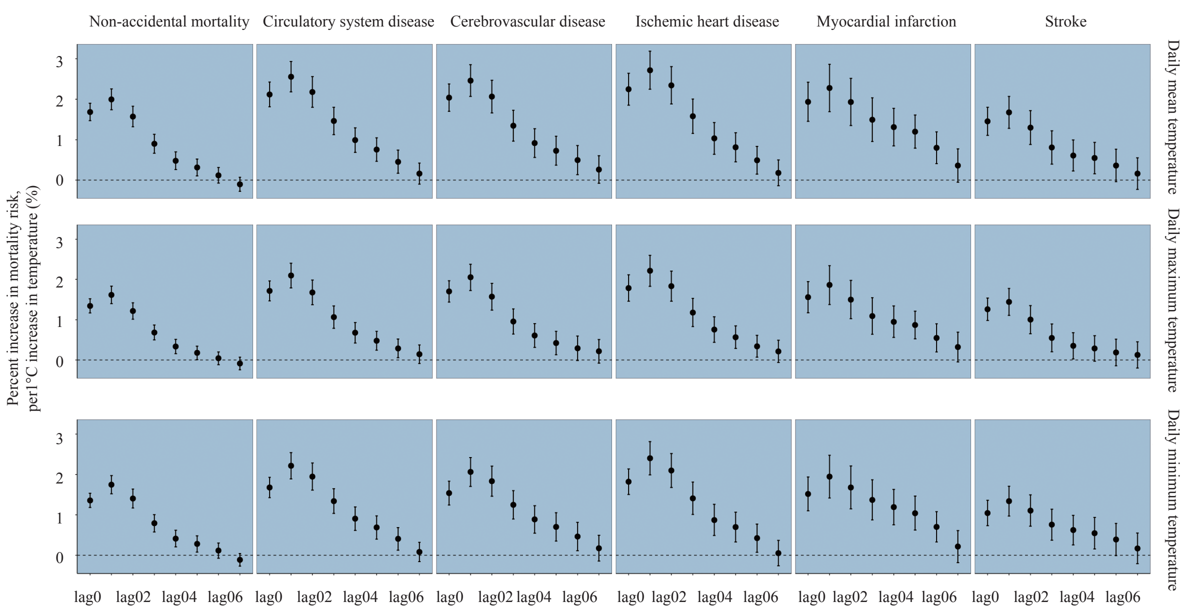

SUPPLEMENTARY FIGURE S2. Percent increase in mortality risk due to lagged effect of heat exposure for summer months in 2013 to 2018 nationwide.

SUPPLEMENTARY TABLE S1. Descriptive analysis of daily cause-specific mortality and meteorological data for the summer months in 2013 to 2018 at four climatic zones.

Item	Subtropics	Warm-temperature zone	Middle-temperature zone	Plateau climatic zone
Number of counties	42	71	15	2
Causes of death (Mean ± SD)				
Non-accidental mortality	9 ± 6	9 ± 7	8 ±6	1 ± 1
Circulatory system disease	4 ± 3	4 ± 4	4 ± 3	1 ± 1
Cerebrovascular disease	2 ± 2	2 ± 2	2 ± 2	0 ± 1
Ischemic heart disease	1 ± 1	2 ± 2	2 ± 2	0 ± 0
Myocardial infarction	1 ± 1	1 ± 1	1 ± 1	0 ± 0
Stroke	1± 1	1±2	1 ± 1	0 ± 1
Meteorological factors (Mean ± SD)				
Daily mean temperature (℃)	26 ± 4	24 ± 4	21 ± 5	11 ± 4
Daily maximum temperature (℃)	29 ± 4	29 ± 4	26 ± 5	16 ± 5
Daily minimum temperature (℃)	22 ± 4	20 ± 4	16 ± 5	6 ± 5
Daily mean relative humidity (%)	80 ± 10	68 ± 15	64 ± 20	69 ± 16

SUPPLEMENTARY TABLE S2. Z test of different heat temperature indicators on cause-specific mortality risk for the summer months in 2013 to 2018 nationwide.

Item	Percent increase in mortality risk (%)(95%CI)					
	Non-accidental mortality	Circulatory system disease	Cerebrovascular disease	Ischemic heart disease	Myocardial infarction	Stroke
Indicator						
Daily mean temperature*	2.00 (1.74–2.25)	2.56 (2.18–2.93)	2.46 (2.07–2.85)	2.71 (2.25–3.19)	2.28 (1.70–2.86)	1.67 (1.28–2.07)
Daily maximum temperature	1.61 (1.40–1.83) †	2.10 (1.79–2.41) †	2.05 (1.72–2.38) †	2.21 (1.82–2.60) †	1.86 (1.37–2.35) †	1.44 (1.11–1.77) †
Daily minimum temperature	1.75 (1.52–1.97) †	2.21 (1.89–2.54) †	2.06 (1.71–2.42) †	2.40 (1.99–2.81)	1.94 (1.42–2.47) †	1.34 (0.97–1.71) †

* Daily mean temperature as a reference.

† Z test: p value<0.05.

SUPPLEMENTARY TABLE S3. Summary estimates of sensitivity analysis for daily mean temperature and non-accidental mortality.

Item	No. of Counties	Percent increase in mortality risk (%)(95%CI)
The main analysis		
df_{time}=3	130	2.00 (1.74–2.25)
Alternative degrees of freedom		
df_{time}=2	130	1.51 (1.29–1.74)
df_{time}=4	130	1.94 (1.70–2.18)
Adjusted by adding air pollutants		
$PM_{2.5}$	130	2.19 (1.89–2.49)
O_3	130	2.08 (1.79–2.38)

Preplanned Studies

Antibiotics in Drinking Water and Health Risks — China, 2017

Jia Lyu[1]; Yongyan Chen[1]; Lan Zhang[1,#]

Summary

What is already known about this topic?

Antibiotic contaminations in the environment are understood to pose human health risks including disturbing the microbiome in the human body and producing antibiotic-resistant bacteria, which pose serious public health risks. Antibiotics have been detected in aquatic environments and drinking water worldwide.

What is added by this report?

Contamination levels of antibiotics in raw, finished, and tap water were investigated systematically, to the best of our knowledge, in major Chinese water basins. Multiple antibiotic contaminations in raw water and their incomplete removal during water-treatment processes results in human exposure to antibiotics via drinking water. Human exposure to such antibiotics and its health risks were evaluated in this study.

What are the implications for public health practice?

This study highlights the need to strengthen management of antibiotic exposure from drinking water. A multisectoral action plan at the national level is required to curb the effects of environmental antibiotic pollution.

Antibiotic contamination in the environment has become a global issue attracting substantial attention from the general public. Intake of antibiotics from the environment by food and drinking water may disturb the microbiome, especially the gut microbiota in the human body (*1*). More importantly, antibiotic residues in the environment have the potential to produce antibiotic-resistant bacteria (ARB), which pose serious public health risks (*2*). Antibiotics in aquatic environments and drinking water have been detected in China (*3*), but studies measuring exposure to antibiotics in drinking water and associated health risks are limited. In this study, contamination levels of antibiotics in raw, finished, and tap water were investigated systematically for the first time in major Chinese water basins during the winter and summer of 2017. Human exposure and its health risks were also evaluated. Study results indicated that multiple antibiotics were generally detected in raw water from major Chinese water basins. Concentrations of detected antibiotics were at the nanogram per liter level, which were similar to those in other developed countries (*3*). Based on toxicity data or data on therapeutic approaches in the literature, health risk quotients (HRQs) for water basins from exposure to antibiotics via drinking water ranged from 5.1×10^{-7} to 2.2×10^{-3}, exhibiting spatial and seasonal variations. The HRQs quantified in this study were at an acceptable risk level (HRQs were much lower than 1), but the risks from antibiotic resistance are not well understood and should be researched further. Antibiotic contaminations in environments can induce environmental antibiotic-resistant bacteria (eARB) and horizontal gene transfer (HGT) between eARB and pathogens with antibiotic-resistance (pARB), which has been identified as a major threat to public health. A multisectoral action plan at the national level is required to curb the effects of environmental antibiotic pollution.

Contamination data on antibiotics were extracted from a project investigating emerging contaminants in drinking water in major Chinese river basins. In the project, the levels of contamination of 57 pharmaceuticals in raw, finished, and tap water from representative drinking water treatment plants (DWTPs) located in six large river basins, inland river areas, and key lake and reservoir areas of China during the winter and summer of 2017 were investigated. The water basins and areas investigated in the project included the Yangtze River, Yellow River, Pearl River, Songhua River, Huaihe River, Liaohe River, Northwest Rivers, Taihu Lake, Dianchi Lake, Chaohu Lake, Three Gorges Reservoir, and Danjiangkou Reservoir. Pharmaceuticals were analyzed by an ultra-performance liquid chromatography–tandem mass spectrometer (UPLC–MS/MS), as described in detail in a previous study (*3*). Based on a literature review and preliminary survey results, 21 antibiotics (Table 1) commonly used for human and animals were selected

TABLE 1. Detection rates and concentrations of antibiotics in raw water from major Chinese water basins during the winter and the summer of 2017.

Sub-category	Antibiotic	Usage*	Detection rate in winter(n=54)	Concentration in winter	Detection rate in summer(n=54)	Concentration in summer
			Percentage (%)	Median (P_{25}, P_{75}) (ng/L)	Percentage (%)	Median (P_{25}, P_{75}) (ng/L)
β-lactams (βLs)	Penicillin G	1	0 (0/54)	ND	0 (0/54)	ND
	Cloxacillin	1	1.9 (1/54)	11.0	1.9 (1/54)	1.2
	Cephalecxin	1	38.9 (21/54)	5.1 (2.1, 9.9)	9.3 (5/54)	0.6 (0.5, 0.8)
	Ceftiofur	2	0 (0/54)	ND	0 (0/54)	ND
Macrolides (MLs)	Clarithromycin	1	13.0 (7/54)	1.1 (1.0, 1.5)	68.5 (37/54)	0.3 (0.2, 0.6)
	Roxithromycin	1	77.8 (42/54)	1.0 (0.7,1.8)	83.3 (45/54)	0.8 (0.4, 1.7)
	Tylosin	2	3.7 (2/54)	2.8 (2.7, 2.9)	11.1 (6/54)	10.0 (2.7, 83.0)
Sulfonamides (SAs)	Sulfapyridine	2	33.3 (18/54)	0.8 (0.6, 1.1)	57.4 (31/54)	0.2 (0.1, 0.4)
	Sulfadiazine	1	50.0 (27/54)	2.5 (1.6, 3.2)	88.9 (48/54)	0.7 (0.2, 1.6)
	Sulfamethoxazole	1	88.9 (48/54)	9.1 (6.3, 14.0)	90.7 (49/54)	2.4 (1.5, 4.2)
	Sulfathiazole	1	1.9 (1/54)	98.0	37.0 (20/54)	0.1 (0.1, 0.4)
	Sulfamethazine	1	46.3 (25/54)	2.2 (1.8, 11.0)	53.7 (29/54)	1.0 (0.4, 2.6)
	Sulfaquinoxaline	2	7.4 (4/54)	1.1 (0.8, 1.3)	18.5 (10/54)	0.2 (0.1, 0.4)
	Sulfadoxin	2	0 (0/54)	ND	24.1 (13/54)	0.1 (0.1,0.2)
	Trimethoprim	1	27.8 (15/54)	2.5 (1.9, 2.7)	48.1 (26/54)	0.7 (0.4, 1.0)
Quinolones (QNs)	Norfloxacin	1	0 (0/54)	ND	0 (0/54)	ND
	Ciprofloxacin	1	0 (0/54)	ND	14.8 (8/54)	1.8 (0.8, 2.9)
	Enrofloxacin	2	0 (0/54)	ND	20.4 (11/54)	1.4 (0.9, 7.5)
	Ofloxacin	1	0 (0/54)	ND	5.6 (3/54)	1.3 (1.2, 29.0)
	Clinafloxacin	2	0 (0/54)	ND	0 (0/54)	ND
	Sarafloxacin	2	1.9 (1/54)	1.9	59.3 (32/54)	0.4 (0.2, 0.7)
The number of detected antibiotics			13		17	

* 1=Use for both human and animals; 2=Use for animals only.
Abbreviation: ND=not detected.

for analysis in this study. Removal rates (percent eliminated) of antibiotics in DWTPs were calculated by dividing the removal concentration by the concentration in raw water, and the removal concentration was obtained through subtracting finished water concentration from raw water concentration*.

The HRQ for each water basin was the sum of the HRQs for each antibiotic detected in tap water. An HRQ for each antibiotic was calculated by dividing its average daily potential dose (ADD) by the acceptable daily intake (ADI) or risk-specific dose (RSD)†. The ADI or RSD for each antibiotic was obtained from literature research. When there were more than one ADIs or RSDs for each antibiotic, HRQs were calculated using the most restrictive ADI or RSD (*4*). ADD was the antibiotic exposure dose ingested through drinking and dermal absorption during water consumption, calculated with exposure parameters according to *Chinese Exposure Factor Handbook* and the concentrations of antibiotics in tap water. HRQ above 1 is interpreted as indicating the potential for adverse effects, while HRQ below 1 is interpreted as indicating acceptable risk.

Multiple antibiotics were generally detected in raw water from major Chinese water basins (Table 1), and the detection of antibiotics exhibited seasonal variation. The composition of antibiotic contamination in raw water during the summer was more complex than that during the winter. A total of

* The formula of removal rate of an antibiotic: Removal rate = (C_{raw}-$C_{finished}$)/C_{raw}×100%, where C_{raw} is the concentration of the antibiotic in raw water (ng/L), $C_{finished}$ is the concentration of the antibiotic in finished water in the same DWTP (ng/L).
† HRQs for antibiotic exposure via drinking water were calculated using the concentration of antibiotics in tap water, exposure parameters, and the ADIs or RSDs from literatures. The formulae are presented in the Supplementary Materials available in http://weekly.chinacdc.cn/.

17 antibiotics were detected in raw water during the summer with median detected concentrations ranging from 0.1 ng/L to 10.0 ng/L. Among which, seven antibiotics had detection rates above 50%, with 2 of these used for animals only, and the others used for both humans and animals. A total of 13 antibiotics were detected in raw water during the winter, and only two antibiotics detected had detection rates above 50%.

The removal efficiency of each antibiotic from DWTPs was shown in Figure 1. A total of 17 antibiotics detected in raw water had average removal rates of above 50%. β-lactams had average removal rates above 98% and were rarely detected in finished and tap water. Although macrolides (MLs), sulfonamides (SAs), and quinolones (QNs) had average removal rates of 51%–97%, incomplete removal of these antibiotics by conventional technologies in drinking-water treatment plants leaves antibiotic residues in finished and tap water. A total of 16 antibiotics were detected in finished water, and similar results were observed in tap water.

HRQs for water basins ranged from 4.79×10^{-6} to 2.15×10^{-3} in the summer and from 5.10×10^{-7} to 1.69×10^{-3} in the winter (Table 2). HRQs of human exposure to antibiotics through drinking water exhibited spatial and seasonal variations. Huaihe River and Chaohu Lake basins had HRQs above 10^{-3} during the summer and the main antibiotic residues in drinking water in these areas were ciprofloxacin and sarafloxacin. Songhua River Basin had HRQs above 10^{-3} during the winter and the main antibiotic residues in drinking water were clarithromycin and roxithromycin. Additionally, among six large Chinese water basins investigated, the contamination risks in the Yangtze River and Yellow River basins were mainly from sarafloxacin and clarithromycin. The contamination risk in the Pearl River Basin was mainly attributable to tylosin.

DISCUSSION

Investigation of antibiotic contaminations in raw, finished, and tap water in major Chinese river basins indicated that the general population had been exposed to multiple antibiotics through drinking water. Concentrations of detected antibiotics were at the nanogram per liter level in raw, finished, and tap water samples. Contamination levels were similar to those in other developed countries (*3*). Among these antibiotics detected in tap water, seven were used for animals only including sarafloxacin and tylosin. Sarafloxacin was one of the main risk components of antibiotic contaminant exposure for people in the Huaihe River, Yellow River, and Yangtze River basins. Tylosin was the main risk component in the Pearl River Basin.

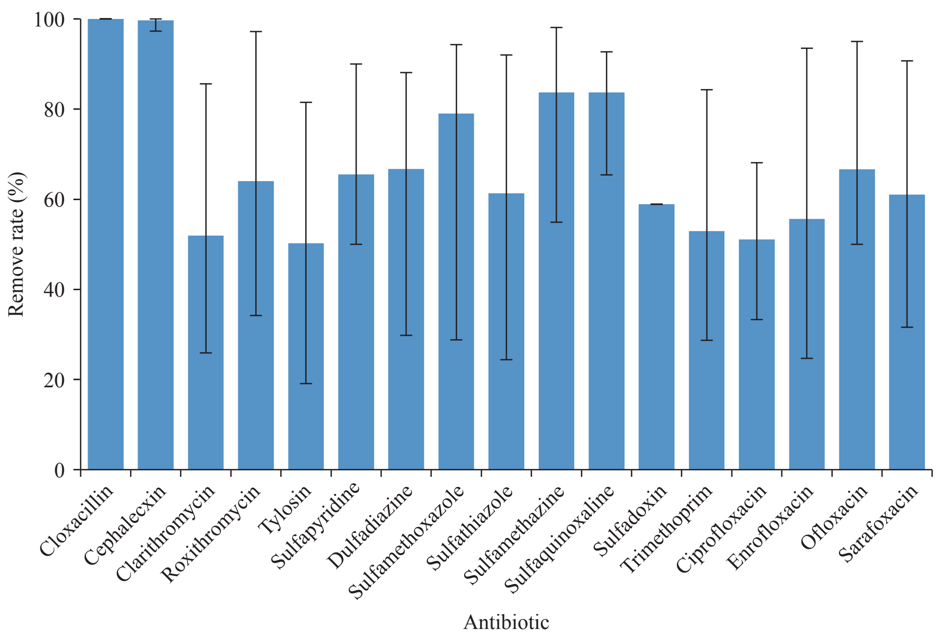

FIGURE 1. Removal efficiency of 17 antibiotics detected in raw water with positive removal rates in the DWTPs. Removal rates (% elimination) were calculated by dividing the removal concentration by the concentration in raw water, and the removal concentration was obtained through subtracting finished water concentration from raw water concentration.

TABLE 2. Health risk quotients of exposures to antibiotics via drinking water for people from major Chinese water basins during the winter and the summer of 2017.

Water Basins	Season	Health risk quotient		
		Minimum	Median	Maximum
Yangtze River (*n*=10)	Winter	8.62×10^{-6}	1.89×10^{-5}	2.57×10^{-5}
	Summer	3.71×10^{-5}	4.19×10^{-5}	1.04×10^{-4}
Yellow River (*n*=10)	Winter	2.33×10^{-5}	4.23×10^{-5}	4.40×10^{-5}
	Summer	7.17×10^{-5}	1.52×10^{-4}	9.67×10^{-4}
Pearl River (*n*=10)	Winter	5.10×10^{-7}	1.33×10^{-6}	1.73×10^{-6}
	Summer	3.33×10^{-4}	5.31×10^{-4}	7.67×10^{-4}
Songhua River (*n*=10)	Winter	9.63×10^{-5}	8.75×10^{-4}	1.69×10^{-3}
	Summer	3.67×10^{-5}	3.08×10^{-4}	3.64×10^{-4}
Huaihe River (*n*=10)	Winter	7.48×10^{-5}	2.83×10^{-4}	3.96×10^{-4}
	Summer	1.09×10^{-3}	1.81×10^{-3}	2.15×10^{-3}
Liaohe River (*n*=10)	Winter	2.83×10^{-5}	3.01×10^{-5}	6.35×10^{-5}
	Summer	1.16×10^{-4}	1.52×10^{-4}	1.80×10^{-4}
Northwest Rivers (*n*=2)	Winter	ND*	ND*	ND*
	Summer	4.79×10^{-6}	4.79×10^{-6}	4.79×10^{-6}
Taihu Lake (*n*=10)	Winter	1.51×10^{-5}	5.73×10^{-5}	1.23×10^{-4}
	Summer	4.40×10^{-5}	7.86×10^{-5}	8.22×10^{-5}
Dianchi Lake (*n*=10)	Winter	2.03×10^{-5}	2.86×10^{-5}	3.00×10^{-5}
	Summer	3.35×10^{-5}	7.16×10^{-5}	3.73×10^{-4}
Chaohu Lake (*n*=10)	Winter	3.74×10^{-5}	6.27×10^{-5}	8.02×10^{-5}
	Summer	2.95×10^{-4}	1.40×10^{-3}	1.44×10^{-3}
Three Gorges Reservoir (*n*=10)	winter	3.71×10^{-5}	9.59×10^{-5}	1.78×10^{-4}
	Summer	1.67×10^{-5}	3.07×10^{-5}	4.20×10^{-5}
Danjiangkou Reservoir (*n*=8)	Winter	3.92×10^{-5}	4.88×10^{-5}	4.92×10^{-5}
	Summer	2.32×10^{-5}	1.62×10^{-4}	2.98×10^{-4}

* No antibiotic was detected in drinking water samples from Northwest Rivers Basin area during the winter.

Antibiotic contaminations in the environment were mainly attributed to the extensive use and emission of antibiotics in livestock farming and aquaculture (*5*–*6*).

The removal rate of each antibiotic in DWTPs investigated in this study showed that conventional purification methods during water treatment cannot remove antibiotics from raw water completely. Similar removal effects of antibiotics were also seen in previous studies (*7*). Incomplete removal during water-treatment processes results in human exposure to antibiotics from contaminated environments via drinking water. Antibiotics can enter an aquatic environment through effluents from sewage treatment plants (STPs) because of the limited removal efficiency from such plants (*8*). In addition to emissions of antibiotics from livestock farming and aquaculture, industrial effluent from drug manufacturing is another major source of antibiotic contamination, contributing high-level contaminations by some antibiotics in surface water and thus in drinking water through water system.

HRQs of antibiotic contaminations in drinking water were less than or equal to 10^{-3} level, which were much lower than 1, indicating an acceptable level of risk from exposure to antibiotics via drinking water. However, these risks from exposure to antibiotics via drinking water varied across water basins and seasons. HRQs above 1×10^{-3} were observed in Huaihe River and Chaohu Lake Basins during the summer and in Songhua River Basin during the winter.

There are three limitations in our analysis. First, contamination data used in this study were collected from representative DWTPs in major river basins, which did not cover all river basins and regions in

China. Hence, study results only represented the population in water-supply areas of these DWTPs. Second, ADIs used in this study to calculate HRQs of antibiotics were derived from the data based on the toxicity of experimental animal or microbiological effects in the literature. There is a lack of study on the adverse effects induced by antibiotics exposure from environments among all age groups and sensitive groups such as children and pregnant women. Finally, antibiotic contaminations in environments can induce eARB (*9*). Previous studies have highlighted the potential for environmental HGT between eARB and pARB, which has been identified as a major threat to public health (*10*). However, the risk of antibiotic resistance is not quantified in this study because of the limited research data. A study on the health risks of environmental antibiotic pollution is crucially needed to provide data to support for risk management in China.

From both human and environmental health perspectives, it is a significant task to establish a systematic project for curbing the effects of environmental antibiotic pollution. A multisectoral action plan at the national level is required: (a) to strengthen the control of antibiotic use in livestock farming and aquaculture, taking steps to reduce usage and emissions of antibiotics at national levels; (b) to improve a standard wastewater discharge system for antibiotic industries and to establish an emission standard for antibiotics to strengthen discharge management; (c) to conduct further research on removal mechanisms of antibiotics by water-treatment technology, exploring the applicability of upgrading treatment processes in STPs and DWTPs; (d) to carry out systematic research on environmental antibiotic pollution and antibiotic resistance; and (e) to conduct research on and investigate antibiotic contamination exposure and health risk assessment among all age groups and sensitive groups.

Conflict of interests: No conflicts of interest were reported.

Acknowledgements: The authors are grateful to the participants and investigators for their involvement in the survey.

doi: 10.46234/ccdcw2020.106

[#] Corresponding author: Lan Zhang, zhanglan@nieh.chinacdc.cn.

[1] China CDC Key Laboratory of Environment and Population Health, National Institute of Environmental Health, Chinese Center for Disease Control and Prevention, Beijing, China.

Submitted: May 16, 2020; Accepted: May 24, 2020

REFERENCES

1. Francino MP. Antibiotics and the human gut microbiome: dysbioses and accumulation of resistances. Front Microbiol 2016;6:1543. http://dx.doi.org/10.3389/fmicb.2015.01543.
2. O’Neill J. Tackling drug-resistant infections globally: final report and recommendations. The Review on Antimicrobial Resistance. 2016. https://amr-review.org/sites/default/files/160525_Final%20paper_with%20cover.pdf.
3. Lv J, Zhang L, Chen YY, Ye BX, Han JY, Jin N. Occurrence and distribution of pharmaceuticals in raw, finished, and drinking water from seven large river basins in China. J Water Health 2019;17(3):477 – 89. http://dx.doi.org/10.2166/wh.2019.250.
4. Leung HW, Jin L, Wei S, Tsui MMP, Zhou BS, Jiao LP, et al. Pharmaceuticals in tap water: human health risk assessment and proposed monitoring framework in China. Environ Health Perspect 2013;121(7):839 – 46. http://dx.doi.org/10.1289/ehp.1206244.
5. Li WH, Shi YL, Gao LH, Liu JM, Cai YQ. Occurrence of antibiotics in water, sediments, aquatic plants, and animals from Baiyangdian Lake in north China. Chemosphere, 2012;89(11):1307 – 15. http://dx.doi.org/10.1016/j.chemosphere.2012.05.079.
6. Li YX, Liu B, Zhang XL, Wang J, Gao SY. The distribution of veterinary antibiotics in the river system in a livestock-producing region and interactions between different phases. Environ Sci Pollut Res 2016;23(16):16542 – 51. http://dx.doi.org/10.1007/s11356-016-6677-2.
7. Cai MQ, Wang R, Feng L, Zhang LQ. Determination of selected pharmaceuticals in tap water and drinking water treatment plant by high-performance liquid chromatography-triple quadrupole mass spectrometer in Beijing, China. Environ Sci Pollut Res 2015;22(3):1854 – 67. http://dx.doi.org/10.1007/s11356-014-3473-8.
8. Li D, Yang M, Hu JY, Ren LR, Zhang Y, Li KZ. Determination and fate of oxytetracycline and related compounds in oxytetracycline production wastewater and the receiving river. Environ Toxicol Chem 2008;27(1):80 – 6. http://dx.doi.org/10.1897/07-080.1.
9. Le Page G, Gunnarsson L, Snape J, Tyler CR. Integrating human and environmental health in antibiotic risk assessment: a critical analysis of protection goals, species sensitivity and antimicrobial resistance. Environ Int 2017;109:155 – 69. http://dx.doi.org/10.1016/j.envint.2017.09.013.
10. Ashbolt NJ, Amézquita A, Backhaus T, Borriello P, Brandt KK, Collignon P, et al. Human health risk assessment (HHRA) for environmental development and transfer of antibiotic resistance. Environ Health Perspect 2013;121(9):993 – 1001. http://dx.doi.org/10.1289/ehp.1206316.

Supplementary Material

Health risk quotient (HRQ) calculation

$$HRQ_{an} = \frac{ADD}{ADI\ or\ RSD} \tag{1}$$

HRQ_{an} is the health risk quotient of an antibiotic, ADD is the average daily potential dose of this antibiotic through drinking and dermal absorption during drinking water consumption [μg/(kg·day)], ADI is the acceptable daily intake [μg/(kg·day)] for noncarcinogenic effects, RSD is the risk-specific dose for carcinogenic effects.

HRQ for each water basin was the sum of the HRQs for each detected antibiotic in tap water from this water basin.

ADI or RSD selection

Acceptable daily intake (ADI) or risk-specific dose (RSD) were found via literature search. ADIs or RSDs of antibiotics were adopted from provisional values established in the literature or derived using previously applied toxicological, microbiological, or therapeutic approaches. When there are more than one ADIs or RSDs for each antibiotic, the most restrictive ADIs or RSDs were selected. The ADIs used for HRQ calculation of each antibiotic are described in Supplementary Table S1.

Evaluation of average daily potential dose (ADD) of each antibiotic

Drinking and dermal absorption are the main intake and uptake routes for human exposure to antibiotics through drinking water consumption.

ADD through intake water (ADD_{dw}) was calculated using Equation S2:

$$ADD_{dw} = \frac{C_{dw} \times IngR \times EF \times ED}{BW \times AT \times 1,000} \tag{2}$$

SUPPLEMENTARY TABLE S1. Acceptable daily intakes (ADIs) or risk-specific dose (RSD) used for Health risk quotient (HRQ) calculation of each antibiotic were selected from literature search.

Antibiotic	ADI or RSD [μg/(kg·day)]	Toxicity endpoint	References
Cephalecxin	10	Microbiological	(*2*)
Clarithromycin	0.2	MIC_{50} on Peptostreptococcus spp.	(*1*)
Roxithromycin	0.4	MIC_{50} on Eubacterum spp.	(*1*)
Tylosin	0.85	MIC_{50} on Bifidobacterium spp. and Clostridium spp.	(*1*)
Sulfapyridine	10	Microbiological	(*3*)
Sulfadiazine	20	reduced fetal bodyweight and C-R length at the next higher dose	(*4*)
Sulfamethoxazole	130	Thyroid tumors in rats	(*1*)
Sulfathiazole	50	Changes in thyroid tissue. a NOEL of 5 mg/kg for the thyroid effects in animal studies	(*1*)
Sulfamethazine	1.6	Thyroid gland follicular adenoma in rats with tumor incidence data	(*1*)
Sulfaquinoxaline	10	Increased thyroid weights at the next higher dose	(*2*)
Sulfadoxin	50	Increased liver weights at the next higher dose	(*2*)
Norfloxacin	14.2	Microbiological	(*4*)
Ciprofloxacin	0.15	Microbiological	(*4*)
Enrofloxacin	6.2	Microbiological	(*3*)
Ofloxacin	3.2	Microbiological	(*4*)
Sarafloxacin	0.3	Microbiological	(*4*)
Trimethoprim	4.2	MIC of the most sensitive species in human gut flora	(*3*)

ADD_{dw} is the average daily potential dose from intake of water [μg/(kg·day)], C_{dw} is the concentration of antibiotics in drinking water (ng/L), IngR is the ingestion rate (L/day), including both direct and indirect ingestion, EF is the exposure frequency (days/year), ED is the exposure duration (years), BW is body weight (kg), and AT is averaging time (days). To reduce uncertainties in exposure variation between different geographical areas, across seasons, and between men and women, the IngR values were used corresponding to area, season, and sex as well as the sex-specific BW value in China according to the *Chinese Exposure Factor Handbook* (China EPA 2009; area, season and sex-specific values are shown in Supplementary Table S2).

SUPPLEMENTARY TABLE S2. IngR values corresponding to area, season and sex in China were selected to calculate ADD_{dw}.

Area	Season	Gender	IngR (L/day)
Liaoning	Winter	Male	1,742
Heilongjiang	Winter	Male	1,881
Jiangsu	Winter	Male	2,267
Anhui	Winter	Male	2,944
Hubei	Winter	Male	1,500
Guangdong	Winter	Male	1,695
Chongqing	Winter	Male	1,215
Sichuan	Winter	Male	1,862
Yunnan	Winter	Male	1,895
Gansu	Winter	Male	2,587
Xinjiang	Winter	Male	2,974
Liaoning	Summer	Male	2,090
Heilongjiang	Summer	Male	2,196
Jiangsu	Summer	Male	3,204
Anhui	Summer	Male	4,063
Hubei	Summer	Male	2,570
Guangdong	Summer	Male	2,411
Chongqing	Summer	Male	2,053
Sichuan	Summer	Male	3,184
Yunnan	Summer	Male	2,719
Gansu	Summer	Male	3,990
Xinjiang	Summer	Male	3,716
Liaoning	Winter	Female	1,425
Heilongjiang	Winter	Female	2,180
Jiangsu	Winter	Female	1,817
Anhui	Winter	Female	2,432
Hubei	Winter	Female	1,366
Guangdong	Winter	Female	1,663
Chongqing	Winter	Female	1,293
Sichuan	Winter	Female	1,691
Yunnan	Winter	Female	1,492
Gansu	Winter	Female	2,050
Xinjiang	Winter	Female	2,086
Liaoning	Summer	Female	1,706

TABLE S2. (Continued)

Area	Season	Gender	IngR (L/day)
Heilongjiang	Summer	Female	1,826
Jiangsu	Summer	Female	2,558
Anhui	Summer	Female	3,423
Hubei	Summer	Female	2,376
Guangdong	Summer	Female	2,347
Chongqing	Summer	Female	2,164
Sichuan	Summer	Female	3,062
Yunnan	Summer	Female	2,203
Gansu	Summer	Female	3,133
Xinjiang	Summer	Female	2,703

ADD through dermal absorption with water use (ADD_{dermal}) was calculated using Equation S3:

$$ADD_{dermal} = \sum_{i=1}^{9} \frac{DA_{event-i} \times SA_i \times EF_i \times ED_i}{BW \times AT_i} \quad (3)$$

ADD_{dermal} is the average daily potential dose through dermal absorption [μg/(kg·day)]. Dermal exposure was calculated from nine daily activities, including washing hands, face, hair, feet; washing vegetables, dishes, and clothes; and bathing and swimming. $DA_{event-i}$ refers to the absorbed dose from one event [μg/cm^2·day)], as calculated using Equation S4 below. SA_i refers to the skin surface area available for contact (cm^2), according to the *Chinese Exposure Factor Handbook* (China EPA 2009; values summarized in Supplementary Table S3. EF_i refers to the exposure frequency (days/year), ED_i to the exposure duration (years), BW to body weight (kg), and AT_i to averaging time (days). $DA_{event-i}$ was calculated as follows:

$$DA_{event-i} = K_p \times C \times T \times 10^{-6} \quad (4)$$

Kp is the permeability coefficient (cm/hr), C is the chemical concentration in water that is in contact with the skin (ng/L), and T is the time of contact (hours/day), which was determined from references on water usage habits in northern and southern China, as summarized in Supplementary Table S4 (*5*–*6*).

It is difficult to obtain permeability coefficients of antibiotics directly from references. Accordingly, we used a model developed by ten Berge (2010) and recommended by Brown et al. (2016) in a study of eight models for calculating Kp, as follows (*7*):

$$\log Kp = 2.80 + 0.66\log Kow0.0056MW \quad (5)$$

where Kow is the octanol/water partition coefficient of the target antibiotic and MW is the molecular weight

SUPPLEMENTARY TABLE S3. The skin surface area available for contact (SA_i) were obtained according to the Chinese Exposure Factor Handbook

SA_i (cm^2)	Hand cleaning	Face and hair cleaning	Foot cleaning	Dish washing	Vegetable washing	Clothes washing	Bathing	Swimming
Male	800	1,300	1,100	800	800	800	17,000	6,300
Female	700	1,200	1,000	700	700	700	15,000	5,700

SUPPLEMENTARY TABLE S4. The time of contact (T, hours/day) was determined from references on water usage habits in northern and southern China.

Time of contact (hours/day)	Hand cleaning	Face and hair cleaning	Foot cleaning	Dishes washing	Vegetable washing	Clothes washing	Bathing	Swimming
Male in South China	0.0500	0.0783	0.0167	0.0000	0.0000	0.0000	0.1750	0.086
Female in South China	0.0667	0.1117	0.0117	0.0850	0.0717	0.0467	0.2083	0.088
Male in Nouth China	0.0627	0.1012	0.0146	0.0115	0.0091	0.0462	0.2553	0.086
Female in Nouth China	0.0614	0.1168	0.0165	0.1606	0.1364	0.3050	0.2424	0.088

SUPPLEMENTARY TABLE S5. Kow and MW of target antibiotics were used to calculate the permeability coefficient (Kp, cm/hr)

Antibiotic	log Kow	MW(g/mol)
Penicillin G	1.83	334.38
Cloxacillin	2.44	435.88
Cephalecxin	0.65	347.39
Ceftiofur	1.60	523.57
Clarithromycin	3.16	747.95
Roxithromycin	2.21	837.05
Tylosin	1.63	916.11
Sulfapyridine	0.35	249.29
Sulfadiazine	2.59	250.27
Sulfamethoxazole	0.89	253.28
Sulfathiazole	0.05	255.32
Sulfamethazine	0.14	278.33
Sulfaquinoxaline	1.68	300.34
Sulfadoxin	0.43	310.33
Norfloxacin	0.46	319.33
Ciprofloxacin	0.28	331.34
Enrofloxacin	0.64	359.40
Ofloxacin	-0.39	371.37
Sarafloxacin	0.57	385.36
Trimethoprim	0.91	290.32

Abbreviation: Kow=octanol water partition coefficient, MW = molecular weight.

(g/mole). Kow and MW of target antibiotics are summarized in Supplementary Table S5.

REFERENCES

1. Leung HW, Jin L, Wei S, Tsui MMP, Zhou B, Jiao L, et al. Pharmaceuticals in tap water: human health risk assessment and proposed monitoring framework in China. Environ Health Perspect 2013;121(7):839 – 846. http://dx.doi.org/10.1289/ehp.1206244.
2. Australian Pesticides and Veterinary Authority. Acceptable daily intakes (ADI) for agricultural and veterinary chemicals used in food producing crops or animals 2018. https://apvma.gov.au/node/26596.
3. Hanna N, Sun P, Sun Q, Li X, Yang X, Ji X, et al. Presence of antibiotic residues in various environmental compartments of Shandong province in eastern China: its potential for resistance development and ecological and human risk. Environ Int 2018;114:131 – 142. http://dx.doi.org/10.1016/j.envint.2018.02.003.
4. Wang H, Wang N, Qian J, Hu L., Huang P, Su M, et al. Urinary antibiotics of pregnant women in eastern China and cumulative health risk assessment. Environ Sci & Tech 2017;51(6):3518 – 3525. http://dx.doi.org/10.1021/acs.est.6b06474.
5. Duan XL, Zhang WJ, Wang ZS, Guo YM, Zhang YS, Zhang JL, et al. Water related activity and dermal exposure factors of people in typical areas of Northern China. Res of Environ Sci 2010;23(1):55 – 61. http://dx.doi.org/10.13198/j.res.2010.01.57.duanxl.009.(in Chinese).
6. Huang C, Ding X, Zhang L, Zhou W. Analysis on drinking water exposure in Wuxi residents. J of Environ Hyg 2017;7(2):95 – 101. http://dx.doi.org/10.13421/j.cnki.hjwsxzz.2017.02.003.(in Chinese).
7. Brown TN, Armitage JM, Egeghy P, Kircanski I, Arnot JA. Dermal permeation data and models for the prioritization and screening-level exposure assessment of organic chemicals. Environ Int 2016;94:424 – 435. http://dx.doi.org/10.1016/j.envint.2016.05.025.

Recollection

Clean Air Actions and Air Quality Improvements — Beijing-Tianjin-Hebei and Surrounding Areas, China, 2013−2019

Shijie Liu[1]; Yangxi Chu[1]; Jingnan Hu[1,#]

Severe air pollution has brought great challenges to the economic and social development of China, and in response, the Action Plan for the Prevention and Control of Air Pollution was issued and a mix of air pollution prevention and control measures has been released since 2013 such as ultra-low emission retrofitting in thermal power industry, dealing with the small coal-fired boilers, household clean heating programs, and severe pollution mitigation . In addition, the National Research Program for Key Issues in Air Pollution Control was conducted for Beijing-Tianjin-Hebei (BTH) and surrounding areas, which supported significant air quality improvements. This paper reviews the main air pollution prevention and control measures released for BTH and surrounding areas. Moreover, the improvements in air quality and the evolution of air pollution characteristics in this region are also evaluated.

Actions to Prevent and Control Air Pollution

Rapid economic growth based on intensive energy consumption over the past decades has led to serious air pollution across China. At the beginning of 2013, Beijing Municipality, Tianjin Municipality, Hebei Province, and some other regions in China suffered from a persistent haze. Large parts of North and East China were ravaged by haze for more than 20 days, which had a severe effect on human health and economic and social development.

In the same year, the Action Plan for the Prevention and Control of Air Pollution was issued by the State Council, which declared the commencement of intensive air pollution prevention and control. A series of laws, regulations and measures were issued or amended, such as the Environmental Protection Law of the People's Republic of China, the Law of the People's Republic of China on the Prevention and Control of Atmospheric Pollution, etc. The National Ambient Air Quality Standard (GB 3095-2012) was also revised identifing the major air pollutants ($PM_{2.5}$, PM_{10}, SO_2, NO_2, CO, and O_3) (*1*). Two additional technical regulations and guidance (HJ 633-2012 and HJ 663-2013) were released to standardize the assessment and management of air quality and provide health guidance to the general public (*2–3*). The so-called "ground-aerial-space" integrated monitoring system was established to comprehensively monitor the atmospheric environment (*4*), including the satellite remote sensing system, the national air quality, regional particulate, and photochemical composition monitoring networks, etc. A mix of emission mitigation measures had been established and implemented since 2013. A seriers of emission standards for key industries have been released or revised. Upgrading and renovation programs for pollution control facilities in key industries have been pushed forward. An ultra-low emission and energy-saving retrofitting of coal-powered venues and pilot programs for clean household heating in northern China were launched. Small coal-fired boilers (below 10 t/h) in urban areas were eliminated. For mobile sources, the standards for gasoline and diesel fuel quality were strengthened twice in five years, and high-emission vehicles, especially heavy-duty diesel trucks, were under strict supervision.

Due to serious air pollution, BTH and surrounding areas were selected as the key region for air pollution prevention and control. In addition to the policies and measures mentioned above, the National Joint Research Center for Tackling Key Problems in Air Pollution Control was established in 2017. More than 2,000 scientists and researchers were organized to investigate the causes of heavy air pollution and provide solutions for 28 cities in BTH and surrounding area (known as "2+26" cities, including Beijing, Tianjin, Shijiazhuang, Tangshan, Baoding, Langfang, Cangzhou, Hengshui, Handan, Xingtai, Taiyuan, Yangquan, Changzhi, Jincheng, Jinan, Zibo, Liaocheng, Dezhou, Binzhou, Jining, Heze, Zhengzhou, Xinxiang, Hebi, Anyang, Jiaozuo, Puyang, and Kaifeng). A total of 28 expert teams were dispatched to "2+26" cities, and investigation on the

"Customized strategy for each city" campaign was conducted. A comprehensive mechanism for responding to heavy pollution was also established for BTH and surrounding areas, including air quality forecast, expert joint-meetings, heavy pollution warnings, instant emission reduction, and supervised enforcement, which significantly improved the capabilities of local governments to tackle the heavy pollution problem.

Trends in Air Quality Improvement

The comprehensive air pollution prevention and control measures have led to sustained improvements in air quality in BTH and surrounding areas (*5–7*). Figure 1 shows the trends of the annual evaluation concentrations for major pollutants, namely the annual average concentrations of $PM_{2.5}$, PM_{10}, SO_2, NO_2, the annual 95^{th} percentile of the daily average concentrations of CO, and the annual 90^{th} percentile of the maximum daily 8-h average (MDA8) concentrations of O_3 (*3*). As some of the cities in Shanxi Province and Henan Province were not included in national air quality monitoring network in 2013 and 2014, the concentrations of CO, O_3 and $PM_{2.5}$ were not measured in those cities. The cities with missing data were listed in Supplementary Table S1. The concentrations of major pollutants, except for O_3, showed continuous decreases from 2013 to 2019. Compared to 2013, the mean annual evaluation concentrations of $PM_{2.5}$, PM_{10}, SO_2, NO_2, and CO in "2+26" cities in 2019 decreased by 50%, 41%, 79%, 20%, and 53%, respectively. SO_2 and CO, with the greatest concentration decrease among basic pollutions in "2+26", showed the remarkable effects of coal consumption control. For Beijing, most notably, the concentration of $PM_{2.5}$ in Beijing dropped from 89.5 μg/m^3 in 2013 to 42 μg/m^3 in 2019.

The Air Quality Index (AQI) also showed similar annual improvements in BTH and surrounding areas as illustrated in Figure 2. From 2013 to 2019, the days of heavy and serious pollution (Grade V and VI according to HJ 633-2012 (2), respectively per year had decreased from 88 days to 20 days on city average. In particular, the days of serious pollution dropped from 31 days in 2013 to 2 days in 2019, reflecting the great progress in emission mitigation efforts in the region. Additionally, days with good and excellent air quality for each year have significantly increased and nearly doubled from 2013 to 2019.

$PM_{2.5}$, PM_{10}, and O_3 are the main pollutants in

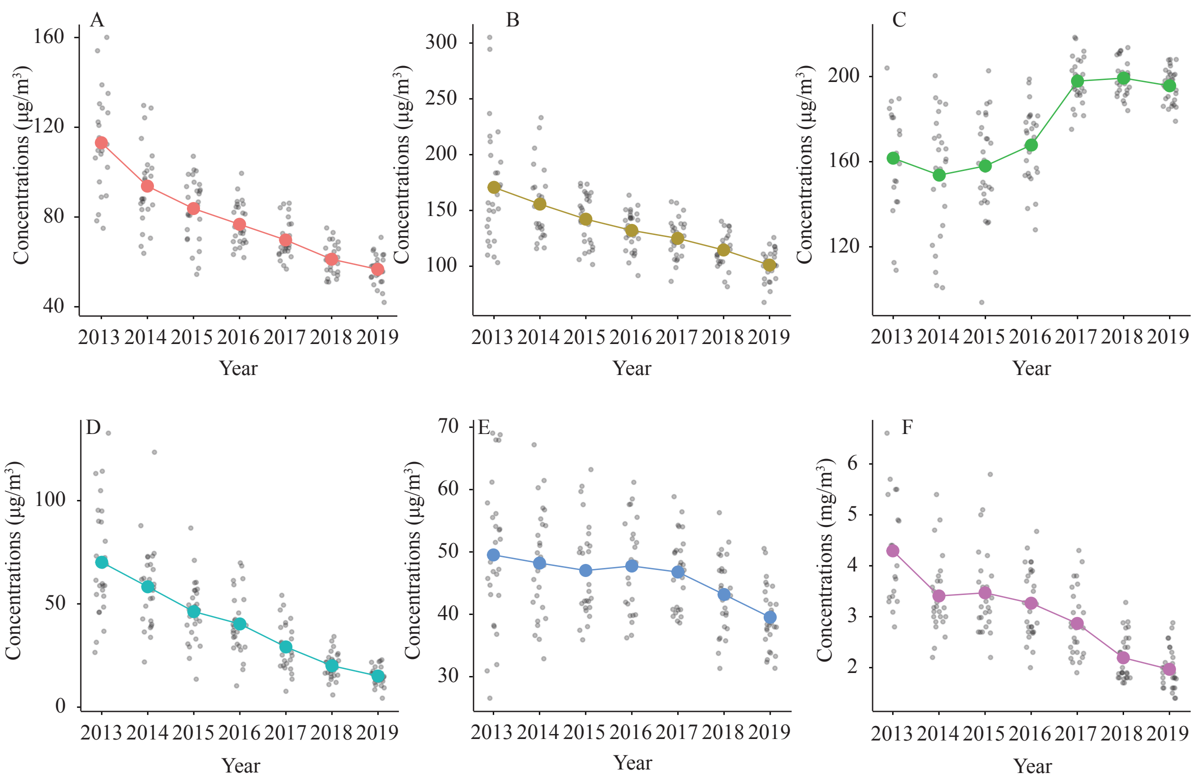

FIGURE 1. Trends of annual evaluations of concentrations of (A) $PM_{2.5}$, (B) PM_{10}, (C) O_3, (D) SO_2, (E) NO_2, and (F) CO in "2+26" cities from 2013 to 2019.

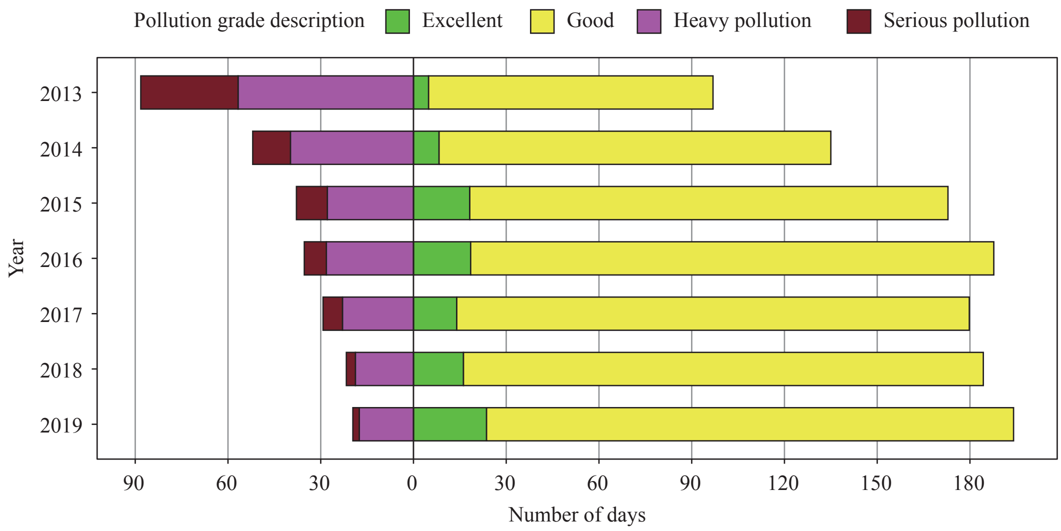

FIGURE 2. Average number of days per year with air quality levels of excellent, good, heavy pollution, and serious pollution in “2+26” cities from 2013 to 2019. The number of days with air quality levels of mild and moderate pollution were not included in the statistics.

polluted days in “2+26” cities. Between 2013 and 2019, the number of polluted days with $PM_{2.5}$ as the chief pollutant decreased continuously (from 189 to 73 days), while the days with O_3 as the chief pollutant increased rapidly from 20 to 80 days. Moreover, O_3 has replaced $PM_{2.5}$ as the most important pollutant in days of chief pollutant from 2018 (Figure 3).

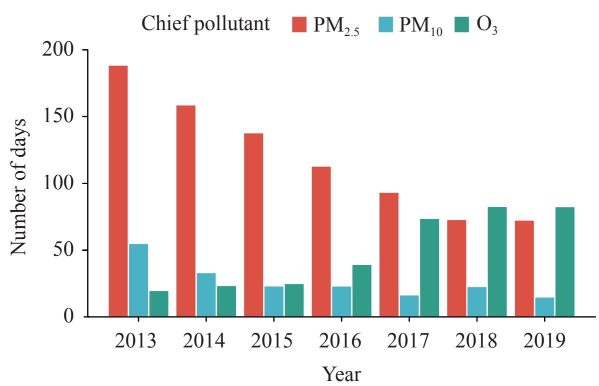

FIGURE 3. The number of air polluted days with different chief pollutants from 2013 to 2019.

Evolution of Air Pollution Characteristics

As the $PM_{2.5}$ concentrations in BTH and surrounding areas decrease, the $PM_{2.5}$ chemical compositions have undergone significant changes over the years. Table 1 shows the changes of major $PM_{2.5}$ components concentrations in the studied region over the years. The most notable change was the reduction in sulfate and organic matter, which decreased by 42% and 31%, respectively, from the 2016–2017 autumn-winter seasons (October 2016–March 2017) to 2018–2019 autumn-winter seasons (October 2018–March 2019). This is due to effective control of coal consumption including household coal replacements, the elimination of small coal-fueled boilers, etc. in BTH and surrounding areas. Emission inventory statistics revealed that households consumed less than 5% of coal in the “2+26” cities but accounted for >20% SO_2 and >30% organic matter emissions. From 2016 to 2018, coal in 8.6 million households were substituted by natural gas and electricity, which reduced emissions of SO_2 and organic matter significantly. On the contrary, the reduction in nitrate concentration (11%) was relatively lower than those of sulfate and organic matter. As a result, the nitrate-to-sulfate mass ratio increased from 1.2 in 2016–2017 autumn-winter seasons to 1.8 in 2018–2019 autumn-winter seasons. Given the decrease in $PM_{2.5}$ concentrations, the mass fraction of nitrate increased to 19.6% in 2018–2019 autumn-winter seasons, and the extent of mass fraction increase (3.4%) is larger than any other species. This highlights the importance of tackling nitrate pollution in the studied region. Ammonium is the major cation in $PM_{2.5}$ to balance the anions charge-wise, and its concentration decreased by 22.4%, which is between the decrease in sulfate and nitrate. Considering the fact that the concentration of ammonia is in excess over those of acidic species (e.g. sulfuric acid and nitric acid gases) in the atmosphere in the studied region, reduction of ammonia emission alone might not lead to substantial air quality improvement without drastic changes (*7*).

TABLE 1. Concentrations and mass fractions of $PM_{2.5}$ components in BTH and surrounding areas in the 2016–2017 and 2018–2019 autumn-winter seasons.

$PM_{2.5}$ component	2016–2017 autumn-winter		2018–2019 autumn-winter	
	Concentration (μg/m^3)	Mass fraction (%)	Concentration (μg/m^3)	Mass fraction (%)
Elemental carbon	4.0	2.6	4.6	4.1
Organic matter	46.3	30.4	31.8	28.3
Nitrate	24.7	16.2	22.1	19.6
Sulfate	21.2	13.9	12.4	11.0
Ammonium	14.5	9.5	11.2	10.0
Chloride	5.9	3.9	4.0	3.6
Crustal matter	4.7	3.1	7.2	6.4
Trace elements	4.2	2.8	2.6	2.3
Others	26.9	17.6	16.5	14.6

Furthermore, studies revealed that the MDA8 surface O_3 concentration during April–September increased in BTH and surrounding areas (*8*). During the seasonal transition period, $PM_{2.5}$ and O_3 complex pollution can occur in the studied region. For instance, on April 30 and May 1, 2020, both daily $PM_{2.5}$ and MDA8 ozone levels exceeded the National Ambient Air Quality Standards (*1–2*) in cities such as Beijing and Tangshan (Supplementary Figure S1 available in http://weekly.chinacdc.cn/). The results show that secondary pollutants such as particulate nitrate, secondary organics, and O_3 had become prominent in recent years, implying the importance and urgency of controlling their precursors such as nitrogen oxides and volatile organic compounds.

Fundings: The study was funded by the National Research Program for Key Issues in Air Pollution Control (DQGG0303, DQGG0307 and DQGG0107). The authors gratefully acknowledge China National Environmental Monitoring Centre for air quality and $PM_{2.5}$ chemical composition monitoring data.

doi: 10.46234/ccdcw2020.107

Corresponding author: Jingnan Hu, hujn@craes.org.cn.

[1] Institute of Atmospheric Environment, Chinese Research Academy of Environmental Sciences, Beijing, China.

Submitted: May 18, 2020; Accepted: May 24, 2020

REFERENCES

1. Ministry of Environmental Protection. GB 3095-2012 Ambient air quality standards. Beijing: China Environmental Science Press, 2016. http://www.mee.gov.cn/ywgz/fgbz/bz/bzwb/dqhjbh/dqhjzlbz/201203/W020120410330232398521.pdf. (In Chinese).
2. Ministry of Environmental Protection. HJ 633-2012 Technical regulation on ambient air quality index (on trial). Beijing: China Environmental Science Press, 2016. http://www.mee.gov.cn/ywgz/fgbz/bz/bzwb/jcffbz/201203/W020120410332725219541.pdf. (In Chinese).
3. Ministry of Environmental Protection. HJ 663-2013 Technical regulation for ambient air quality assessment (on trial). Beijing: China Environmental Science Press, 2013. http://www.mee.gov.cn/ywgz/fgbz/bz/bzwb/jcffbz/201309/W020131105548549111863.pdf. (In Chinese).
4. Liu WQ, Chen ZY, Liu JG, Xie PH. Stereoscopic monitoring technology and applications for the atmospheric environment in China. Chin Sci Bull 2016;61(30):3196 – 207. http://engine.scichina.com/doi/10.1360/N972016-00394. (In Chinese).
5. Cai SY, Wang YJ, Zhao B, Wang SX, Chang X, Hao JM. The impact of the "Air Pollution Prevention and Control Action Plan" on $PM_{2.5}$ concentrations in Jing-Jin-Ji region during 2012-2020. Sci Total Environ 2017;580:197 – 209. http://dx.doi.org/10.1016/j.scitotenv.2016.11.188.
6. Zhang Q, Zheng YX, Tong D, Shao M, Wang SX, Zhang YH, et al. Drivers of improved $PM_{2.5}$ air quality in China from 2013 to 2017. Proc Natl Acad Sci USA 2019;116(49):24463 – 9. http://dx.doi.org/10.1073/pnas.1907956116.
7. Liu MX, Huang X, Song Y, Tang J, Cao JJ, Zhang XY, et al. Ammonia emission control in China would mitigate haze pollution and nitrogen deposition, but worsen acid rain. Proc Natl Acad Sci USA 2019;116(16):7760 – 5. http://dx.doi.org/10.1073/pnas.1814880116.
8. Lu X, Zhang L, Wang XL, Gao M, Li K, Zhang YZ, et al. Rapid increases in warm-season surface ozone and resulting health impact in China Since 2013. Environ Sci Technol Lett 2020;7(4):240 – 7. http://dx.doi.org/10.1021/acs.estlett.0c00171.

SUPPLEMENTARY TABLE S1. The cities missing the concentration data of CO, O_3, and $PM_{2.5}$.

Pollutant	2013	2014
CO	Anyang, Hebi, Jiaozuo, Jincheng, Kaifeng, Puyang, Xinxiang, Yangquan, Changzhi	Hebi, Puyang, Xinxiang
O_3	Anyang, Hebi, Jiaozuo, Jincheng, Kaifeng, Puyang, Xinxiang, Yangquan, Changzhi	Hebi, Puyang, Xinxiang
$PM_{2.5}$	Anyang, Hebi, Jiaozuo, Kaifeng, Puyang, Xinxiang	Hebi, Puyang, Xinxiang

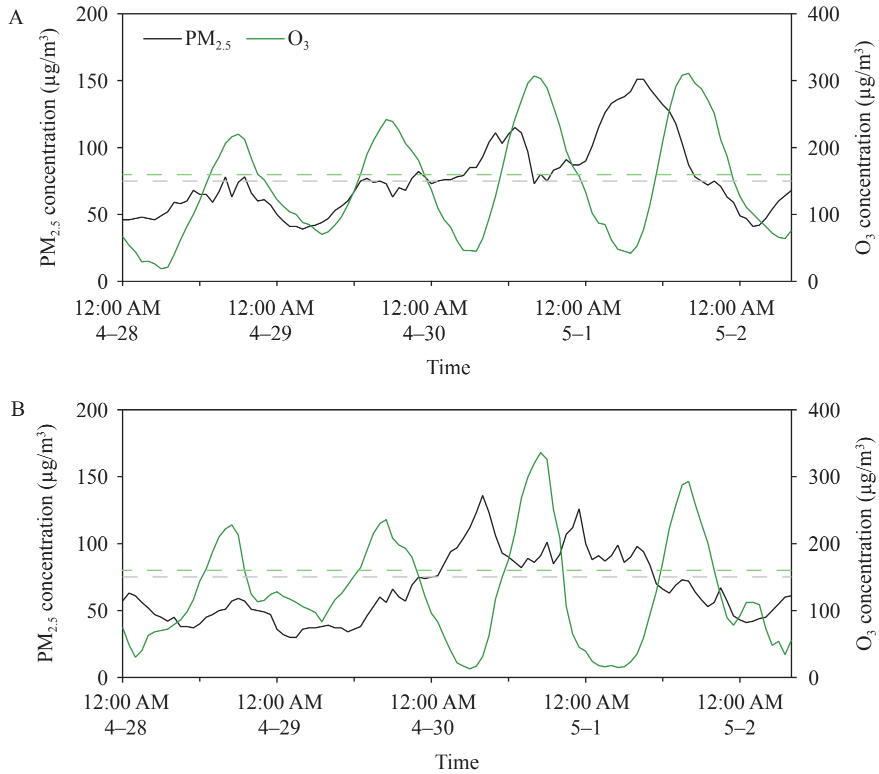

SUPPLEMENTARY FIGURE S1. $PM_{2.5}$ and O_3 hourly concentrations in (A) Beijing and (B) Tangshan from April 28 to May 2, 2020. The grey and light green dashed lines indicate the secondary standards of daily $PM_{2.5}$ concentration (75 μg/m^3) and MDA8 O_3 level (160 μg/m^3), respectively.

Outbreak Reports

Gastroenteritis Outbreak Caused by *Campylobacter jejuni* — Beijing, China, August, 2019

Ying Li[1,&]; Guilan Zhou[2,&]; Peng Gao[1,&]; Yixin Gu[2]; Hairui Wang[2]; Shuang Zhang[1]; Yanchun Zhang[1]; Yuanyuan Wang[1]; Hongbo Jing[1]; Chao He[1]; Guoxin Zhen[1]; Hongmei Ma[1]; Yindong Li[1]; Jianzhong Zhang[2]; Maojun Zhang[2,#]

Summary

What is already known about this topic?

Campylobacter genus bacteria are recognized as some of the leading causes of the bacterial diarrheal illness in both developing and developed countries. Recent pilot surveillance study revealed *Campylobacter* is the most common pathogen in the diarrheal cases using the enhanced filtration methods in Beijing. One outbreak caused by multi-drug resistant *Campylobacter coli* (*C. coli*) was identified in 2018.

What is added by this report?

This is the first identified gastroenteritis outbreak caused by local *Campylobacter jejuni* (*C. jejuni*) infection in Beijing. A total of 14 patients were identified from August 23 to 26, 2019. The epidemiological investigation indicated that all of the patients worked at the same factory and the diarrhea happened after the same meal supplied from one company which service the meal delivery. Fourteen *C. jejuni* isolates were obtained from 12 patients and 2 food workers. Whole Genome Sequencing (WGS) analysis indicated this outbreak was caused by one highly clonal *C. jejuni*.

What are the implications for public health practice?

Campylobacter is the major foodborne pathogen in the world. Surveillance and risk assessment for *Campylobacter* infection particularly for Guillain-Barré Syndrome (GBS) associated *C. jejuni* infection in China should closely monitored.

BACKGROUND

In the afternoon of August 26, 2019, the Shunyi District CDC of Beijing Municipality was informed that several acute gastroenteritis patients visited the Shunyi District Hospital and the Shunyi Chinese Medicine Hospital. The epidemiological investigation was performed by Shunyi CDC. The time of onset of the first patient and the final patient were the afternoon of August 24, 2019 (26 hours after the meal) and the morning of August 26, 2019 (66 hours after the shared meal), respectively.

Totally, 14 patients were identified. These 14 patients showed similar clinical symptoms, including high fever (over 38.5 ℃), diarrhea, abdominal pain, and headache. All of them had watery stool and diarrhea 2 to 10 times per day. According to the epidemic investigation, these 14 patients were workers at the same factory and the diarrhea happened after lunch supplied from a meal delivery company on August 23. Overall, 14 stool samples (7 fresh stool samples and 7 anal swabs) were collected from 14 individual patients, 7 anal swabs were collected from 7 individual workers of the food supplying company, and 18 suspected food samples and 6 samples from the environment of the kitchen were collected. All samples were screened for 10 major enteric pathogens based on the real-time polymerase chain reaction (PCR) methods published previously (*1*).

INVESTIGATION AND RESULTS

Real-time PCR was performed for 10 specific pathogens: *Vibrio cholerae*, *Vibrio parahaemolyticus*, *C. jejuni*, *C. coli*, *Salmonella*, *Shigella*, diarrheagenic *E. coli*, norovirus, rotavirus, and enteric adenovirus. Fourteen samples were positive for *C. jejuni* including 12 samples from 12 patients and 2 samples from 2 food workers, and the other samples were all negative. All samples were negative for other enteric pathogens except for *C. jejuni*.

Campylobacter isolation was performed for all collected samples and species identification was carried out for suspected colonies as previously described (*2*). In total, 80 colonies were obtained from 14 positive samples including 12 patients' samples and 2 food workers' samples. No isolate was obtained from other samples. For each positive sample, one isolate was selected for further investigation, and 14 isolates were picked in total.

Pulsed-field gel electrophoresis (PFGE) was performed for all 14 selected isolates (one isolate was selected from each positive patient and positive food worker) using *Sma* I as described previously (*3*). All of the selected isolates showed an identical PFGE profile (Figure 1).

Antibiotic susceptibility testing for 11 antimicrobials was performed with the agar dilution method as previous study (*1*). All of the selected isolates had the same susceptibility pattern: they were all resistant to nalidixic acid and ciprofloxacin and sensitive to other 9 drugs.

The draft genomes of 13 outbreak associated isolates (11 isolates from 11 individual patients and 2 isolates from 2 food workers) were sequenced. One isolate SF-18Cj008), which was isolated from a local sporadic diarrheal patient, and another isolate ARI1249, isolated from the diarrheal patients in UK, were selected to be enrolled in this study. The WGS of SF-18Cj008 was obtained from our previous study and the WGS of ARI1249 was obtained from the PubMLST database (https://pubmlst.org/bigsdb?db=pubmlst_campylobacter_isolates&page=seqbin&isolate_id=43065). The Whole Genome Single Nucleotide Polymorphisms (wgSNP) was called among the 15 genomes and the Multilocus Sequence Typing (MLST) of the 15 isolates was determined using the online tool on PubMLST website (http://pubmlst.org/campylobacter). The *ad hoc* whole-genome multilocus sequence typing (wgMLST) analysis was performed for 15 *C. jejuni* isolates with fast-GeP (https://github.com/jizhang-nz/fast-GeP) using the annotated ARI1249 genome as reference (*1*). The Sequence Types (STs) of the entire selected 15 isolates all belong to ST-6959. The difference matrix of the allele loci among 15 *C. jejuni* WGSs were presented in Figure 2 and the neighbor-net phylogeny of 15 isolates using SplitsTree4 based on the shared loci was constructed and presented in Figure 3. The outbreak associated 13 isolates were genetically related (≤9 alleles difference). No mutation in 23S rRNA was found and the *gyrA* C257T mutant was identified in the entire 13 outbreak associated isolates which was consisting with the phenotype of drug resistance of the outbreak associated isolate.

DISCUSSION

In this study, 12 *C. jejuni* isolates were obtained from 12 patients. The real-time PCR screening results were consistent with the bacteria culture results. Unfortunately, no isolates were cultured from the two patients of whom the samples were anal swabs and PCR results were also negative. This might be due to an inadequate number of pathogens in the samples. Bacteria culture is time intensive, rapid multi-targets screening using molecular methods is helpful for pathogen identification during the outbreak investigation. This study confirmed that direct real-

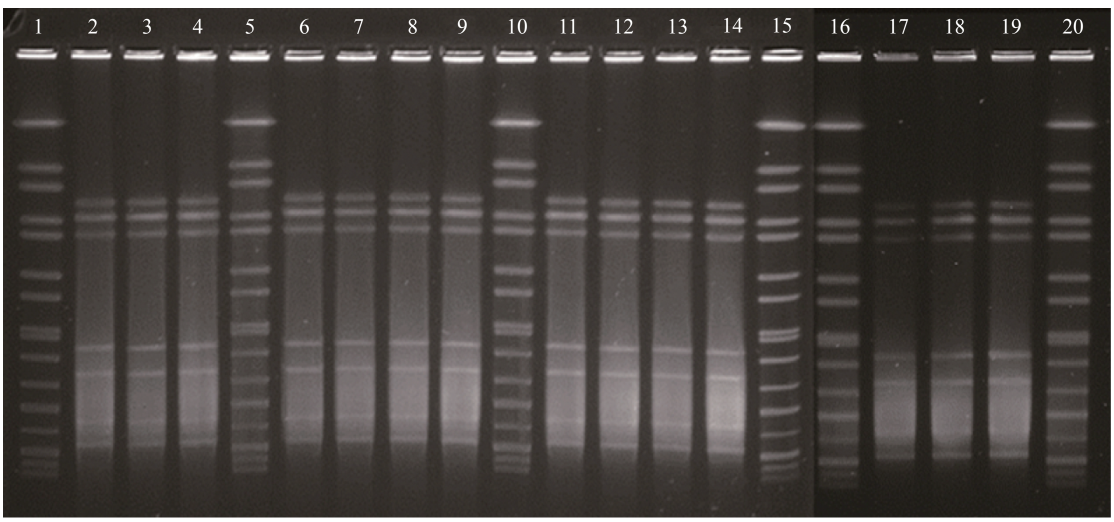

FIGURE 1. Pulsed-field gel electrophoresis (PFGE) analysis with *Sma* I for 14 *Campylobacter jejuni* isolates from 12 patients and 2 food workers. Lanes 1, 5, 10, 15, 16 and 20: refercnce standard H9812; Lanes 2, 3, 4, 6, 7, 8, 9, 11, 12, 13, 14, and 17: *C. jejuni* isolates from 12 patients (isolate 1, 2, 3, 4, 5, 6, 8, 9, 11, 12, 13, and 14); Lanes 18 and 19: *C. jejuni* isolates from 2 food workers (36 and 37). All of the 14 isolates had the same PFGE pattern.

	1.fna	11.fna	12.fna	13.fna	2.fna	3.fna	4.fna	5.fna	6.fna	8.fna	9.fna	36.fna	37.fna	SF-18Cj008.fna	ARI1249.fna
1.fna	0														
11.fna	3	0													
12.fna	4	1	0												
13.fna	2	3	4	0											
2.fna	6	3	4	6	0										
3.fna	5	4	3	5	6	0									
4.fna	6	4	5	4	7	8	0								
5.fna	6	4	5	4	7	8	4	0							
6.fna	6	3	4	6	4	6	7	7	0						
8.fna	5	3	4	6	6	7	7	5	6	0					
9.fna	8	5	6	8	8	8	9	5	8	6	0				
36.fna	8	5	6	8	8	8	9	5	8	6	0	0			
37.fna	8	5	2	4	3	3	5	5	3	4	6	3	0		
SF-18Cj008.fna	59	57	58	58	57	58	56	57	59	57	59	57	56	0	
ARI1249.fna	130	133	134	130	134	135	130	131	136	134	135	135	134	127	0

FIGURE 2. Difference matrix for alleles of the wgMLST with Fast-GeP analysis. Allele sequences were searched with BLAST+ (identity threshold ≥80). ARI1249 was used as the reference genome. The number of the loci in the reference genome was 1,667. The number of loci shared by the 15 genomic sequences was 1,649 and the number of the shared-loci that was found identical was 1,484. The shared-loci that was used to construct distance difference matrix was 1,644 (160 were polymorphic). Five shared-loci were excluded because of hypothetical gene duplication and 18 loci were excluded because of incomplete information (missing, truncation or containing nucleotide ambiguity). The horizontal and vertical columns of the matrix represent the isolates name. The number in the matrix indicated the different alleles numbers between the isolates in the horizontal and vertical. columns. The horizontal and vertical columns of the matrix represent the isolates name. The number in the matrix indicated the different alleles numbers between the isolates in the horizontal and vertical columns.

time PCR examination for *Campylobacter* from the stool sample of diarrheal patients is useful (*4*).

PFGE is useful for bacteria outbreak investigation (*5*). Recently, the WGS for bacterial pathogens become cheaper and faster. The bioinformatics' analysis based on the WGS is crucial for both the epidemic and outbreak investigation (*6*). The ST of the isolate could be reached in real-time with the WGS using the in silico MLST analysis. WgSNP and wgMLST analysis were useful to recognize the genetic distance between the isolates. In this study, the fast-GeP analysis was an effective tool to identify the very closely related *Campylobacter* isolates; it is useful for *Campylobacter* outbreak investigation based on the WGS (*7*). Both the genotyping and antibiotics analysis results indicated this gastroenteritis outbreak was caused by one highly clonal *C. jejuni*.

The isolates from two food workers were of the same genotype as the patients. According to their health history, they did not have significant clinical symptoms. We do not know if they ate the same food as the patients on August 23 or if the bacteria they carried contaminated the foods they cooked. There was a report that *C. jejuni* could colonize in the human gut for extended periods of time (*8*), and there is chance the food workers may contaminate the food during preparation. Unfortunately, we did not get any more samples from any of the food workers for continued bacteria culture.

Recently, the accelerated pace of life may dramatically increase use of meal delivery in major cities and may subsequently increase the risk of infection or food poisoning caused by foodborne pathogens. With an enhanced filtration method, *Campylobacter* was recognized as the leading causes of bacterial diarrhea in Beijing (*1*,*2*,*4*). One gastroenteritis outbreak caused by *C. coli* infection was identified last year (*1*), and this was the first identified

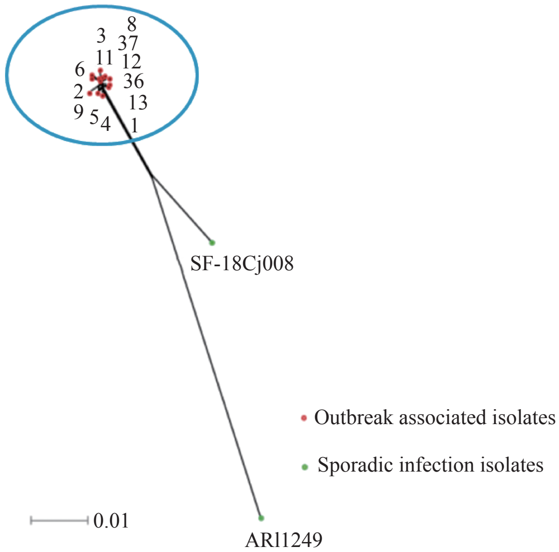

FIGURE 3. Neighbor-net phylogeny for alleles of cgMLST loci of 15 *C. jejuni* isolates. All of these 15 isolates were belonging to ST-6959. Red points representing the outbreak associated 13 isolates (isolate 1, 2, 3, 4, 5, 6, 8, 9, 11, 12, 13, 36 and 37) and green points representing two sporadic isolates (SF-18Cj008 and ARI1249), one from local diarrheal patient, and another one from a diarrheal patient in UK. The blue circle representing the outbreak cluster.

gastroenteritis outbreak caused by local *C. jejuni* infection in Beijing.

In addition to enteritis, *C. jejuni* infection can also cause GBS. Recently, 36 GBS patients outbreak caused by preceding *C. jejuni* infection were reported (*9–10*). According to our previous study, the serotype (HS:41) of this GBS outbreak associated *C. jejuni* strain was also identified from the sporadic diarrheal patient in Beijing. Pathogen surveillance and the risk assessment for *Campylobacter* infection particularly for GBS associated *C. jejuni* infection should be closely monitored.

Acknowledgments: We thank Shunyi CDC colleagues participating in the outbreak investigation; we are grateful to the help from Dr. Ji Zhang in New Zealand for the bioinformatics' analysis.

Fundings: This work was supported by National Key Scientific and Technology Project (2018ZX 10305409 and 2018ZX10712-001).

doi: 10.46234/ccdcw2020.108

Corresponding author: Maojun Zhang, zhangmaojun@icdc.cn.

[1] Shunyi District Center for Disease Control and Prevention, Beijing, China; [2] State Key Laboratory of Infectious Disease Prevention and Control, National Institute for Communicable Disease Control and Prevention, Chinese Center for Disease Control and Prevention.
[&] Joint first authors.

Submitted: December 20, 2019; Accepted: April 03, 2020

REFERENCES

1. Li Y, Gu YX, Lv JC, Liang H, Zhang J, Zhang S, et al. Laboratory study on the gastroenteritis outbreak caused by a multidrug-resistant *Campylobacter coli* in China. Foodborne Pathog Dis 2020;17(3):187 – 93. http://dx.doi.org/10.1089/fpd.2019.2681.
2. Li Y, Zhang S, He M, Zhang YC, Fu YY, Liang H, et al. Prevalence and molecular characterization of *Campylobacter* spp. isolated from patients with diarrhea in Shunyi, Beijing. Front Microbiol 2018;9:52. http://dx.doi.org/10.3389/fmicb.2018.00052.
3. Zhang MJ, Gu YX, He LH, Ran L, Xia SL, Han XS, et al. Molecular typing and antimicrobial susceptibility profiles of *Campylobacter jejuni* isolates from North China. J Med Microbiol 2010;59(10):1171 – 7. http://dx.doi.org/10.1099/jmm.0.022418-0.
4. Liang H, Wen ZY, Li Y, Duan YX, Gu YX, Zhang MJ. Comparison of the filtration culture and multiple real-time PCR examination for *Campylobacter* spp. from stool specimens in diarrheal patients. Front Microbiol 2018;9:2995. http://dx.doi.org/10.3389/fmicb.2018.02995.
5. Davis KR, Dunn AC, Burnett C, McCullough L, Dimond M, Wagner J, et al. *Campylobacter jejuni* infections associated with raw milk consumption--Utah, 2014. MMWR Morb Mortal Wkly Rep 2016;65(12):301-5. https://www.cdc.gov/mmwr/volumes/65/wr/mm6512a1.htm.
6. Oakeson KF, Wagner JM, Rohrwasser A, Atkinson-Dunn R. Whole-genome sequencing and bioinformatic analysis of isolates from foodborne illness outbreaks of *Campylobacter jejuni* and *Salmonella enterica*. J Clin Microbiol 2018;56(11):e00161-18. https://jcm.asm.org/content/56/11/e00161-18.
7. Zhang J, Xiong YW, Rogers L, Carter GP, French N. Genome-by-genome approach for fast bacterial genealogical relationship evaluation. Bioinformatics 2018;34(17):3025 – 7. http://dx.doi.org/10.1093/bioinformatics/bty195.
8. Bloomfield SJ, Midwinter AC, Biggs PJ, French NP, Marshall JC, Hayman DTS, et al. Long-term colonization by *Campylobacter jejuni* within a human host: evolution, antimicrobial resistance, and adaptation. J Infect Dis 2018;217(1):103 – 11. http://dx.doi.org/10.1093/infdis/jix561.
9. Zhang MJ, Li Q, He LH, Meng FL, Gu YX, Zheng MH, et al. Association study between an outbreak of Guillain-Barre syndrome in Jilin, China, and preceding *Campylobacter jejuni* infection. Foodborne Pathog Dis 2010;7(8):913 – 9. http://dx.doi.org/10.1089/fpd.2009.0493.
10. Zhang MJ, Gilbert M, Yuki N, Cao FF, Li JJ, Liu HY, et al. Association of Anti-GT1a Antibodies with an outbreak of Guillain-Barré syndrome and analysis of ganglioside mimicry in an associated *Campylobacter jejuni* strain. PLoS One 2015;10(7):e0131730. http://dx.doi.org/10.1371/journal.pone.0131730.

Perspectives

Urgent Need to Ratify National Legislation Banning Smoking in Public Places

Yuan Jiang[1,#]

China produces 40% of the world's cigarettes (*1*) and has more than 300 million smokers (*2*). How to control smoking is still a serious problem. Smoking damages people's health and increases the burden of medical expenses of the whole society. In order to promote the construction of a healthy China and improve people's health level, the Chinese government issued the outline of "Healthy China 2030" in 2016, which proposed specific measures and objectives for smoking control work: comprehensively promote the implementation of tobacco control, increase the intensity of tobacco control, and use tax and price, law and other means to improve the effectiveness of smoking control. Carry out in-depth tobacco control publicity and education. Actively promote the construction of smoke-free environment and strengthen the supervision and law enforcement of smoke control in public places. We will promote the work of banning smoking in public places and gradually implement a comprehensive ban on smoking in indoor public places. Government leaders should take the lead in banning smoking in public places and build government building into smoke-free one. Strengthen smoking cessation services. By 2030, the adult smoking rate will be reduced to 20% (*3*).

In 2018, China's adult smoking rate was 26.6%, which will be reduced by 6.6 percentage points in 11 years, that is to say, an average annual decrease of 0.6 percentage points. Levy used the SimSmoke model to simulate the implementation of various control policies and their effects (*4*). The results showed that to achieve the Healthy 2030, Framework Convention on Tobacco Control (FCTC) should be fully implemented.

FCTC is the first public health treaty of WHO, it focus on control the prevalence of tobacco from both sides of supply and demand and protect the health of people. Article 8 requires that within five years after ratify, the parties shall adopt legislation to achieve a comprehensive ban on smoking in public places. Although FCTC has been ratified for 14 years in China, there are still no national laws and regulations on tobacco control. By January 2020, more than 20 cities have implemented local regulations on tobacco control, but only 13 cities including Beijing, Shanghai, Shenzhen etc covering about 10% of the national population which meet the requirements of FCTC.

Implement is another important issue after law ratify. Even in Beijing, compared with other cities that have legislation to carry out International Tobacco Control Policy Evaluation projects, the exposure rate of second-hand smoke in indoor workplaces and public places has not decreased to the level of other cities (*5*), but these cities are still very different from the national level (Table 1). After the local laws came into force in Beijing, the adult smoking rate dropped by 1.1 percentage points, and then continued to drop by 2 percentage points in the next two years. It decreased by

TABLE 1. Smoking rate (%) and secondary smoking exposure rate (%) in China, Beijing and Shanghai.

Rate	China			Beijing			Shanghai		
	2010	2015	2018	2014	2016	2019	2016	2017	2018
Adult Smoking Rate	28.1	27.7	26.6	23.4	22.3	20.3	21.0	20.2	19.9
Exposure rate of SHS									
Indoor Working Place	63.3	54.3	50.9	35.7	27.0	27.0	26.1	17.3	17.3
Government Building	54.8	38.1	31.1	19.7	10.8	8.6	11.0	5.3	10.0
Health Facility	37.9	26.9	24.4	12.8	6.2	6.6	11.0	7.5	4.2
Primary and Middle School	36.9	17.2	23.4	32.8	19.1	4.8	17.3	10.9	7.7
Restaurant	88.5	76.3	73.3	65.7	32.5	42.5	44.3	22.8	28.1

3.1 percentage points in four years (*6*–*7*). The adult smoking rate in Shanghai decreased by 19.9 in 2018 from 21.0% in 2016 before the amendment of the law (*8*–*10*) while that in China, including these legislative cities, dropped from 28.1% in 2010 to 26.6%, down 1.5 percentage points in eight years. The average annual decline is less than 0.2 percentage points (*2*).

14 years after ratify FCTC, only 13 cities have issued comprehensive ban smoking laws. If we follow this schedule, it will be difficult to achieve the goal of "total ban on smoking in indoor public places" and "reduction of smoking rate to 20% for people over 15 years old" by 2030. At present, there are 334 cities with legislative right in China. Compared with these 13 cities, the basis of tobacco control in cities without legislation is weak, and tobacco control laws and regulations are often not the priority areas of local legislation. Even if we start the legislative process, we will encounter the interests of all parties and difficulties in resistance. Based on the analysis of the law revision process in Hangzhou in 2018, under the various departments conflicts of interests, the new draft law (first review draft) has only two improvements compared with that before the revision, one is the expansion of the legal coverage, including rural areas, the second is the change from a single law enforcement mode to a multi-department law enforcement mode, and the most core "comprehensive smoke-free" was not included (*11*). If these 300 cities legislate one by one, the efficiency is low, the progress is slow, and the cost is huge. It is difficult to achieve the goal by 2030.

In order to achieve the goal of "Healthy China 2030" and protect more people from second-hand smoke, China should pass national smoking ban legislation in public places as soon as possible, and at the same time speed up the implementation of the law in an all-round way to ensure the realization of the goal of healthy China 2030.

doi: 10.46234/ccdcw2020.114

Corresponding author: Yuan Jiang, jiangyuan88@vip.sina.com.

[1] Tobacco Control Office, Chinese Center for Disease Control and Prevention, Beijing, China.

Submitted: May 09, 2020; Accepted: May 22, 2020

REFERENCES

1. Jiangsu Tobacco Company. What you don't know about cigarette cold knowledge China consumes 40% of the world's tobacco. 2019. https://www.cnxiangyan.com/zhishi/15761.html.[2020-05-12]. (In Chinese).
2. China CDC. 2018 China adult tobacco survey. 2019. http://www.chinacdc.cn/jkzt/sthd_3844/slhd_4156/201908/t20190814_204616.html.[2020-05-18]. (In Chinese).
3. Xinhua News Agency. The State Council of the CPC Central Committee issued the outline of "healthy China 2030". 2016. http://www.gov.cn/xinwen/2016-10/25/content_5124174.htm.[2020-05-16]. (In Chinese).
4. Levy D, Rodríguez-Buño RL, Hu TW, Moran AE. The potential effects of tobacco control in China: projections from the China SimSmoke simulation model. BMJ 2014;348:g1134. http://dx.doi.org/10.1136/bmj.g1134.
5. China CDC. ITC Project China Survey Report: the first to fifth round ofresearchfindings(2006-2015).2017.http://www.chinacdc.cn/jkzt/sthd_3844/slhd_4156/201706/t20170601_143687.html. [2020-05-16]]. (In Chinese).
6. Beijing Municipal Health Commission. Beijing population tobacco survey report: adult tobacco survey report. 2019. http://wjw.beijing.gov.cn/xwzx_20031/xwfb/201912/t20191227_1521991.html.[2020-05-17]. (In Chinese).
7. Jiang RJ. The results of the third Beijing Adult Tobacco Survey revealed that 3.365 million adults smoked in Beijing. 2019. https://www.cn-healthcare.com/article/20191227/content-528004.html. . [2020-05-12]. (In Chinese).
8. Shanghai Release. Shanghai adult smoking rate declines, secondhand smoke exposure gradually improves!. 2018. https://mp.weixin.qq.com/s/w7SD0cxd-zrhkgqe2pdPPA.[2020-05-16]. (In Chinese).
9. Chen D, Jiang YY, Wei XX, Wang J, Le KL, Li M, et al. Cognition of tobacco exposure and tobacco harm in Shanghai residents in 2016. Shanghai J Prev Med 2018;30(8):689 – 93. http://dx.doi.org/10.1016/S1470-2045(17)30041-4. (In Chinese).
10. Shanghai Release. Tomorrow is world no tobacco day! Shanghai adult smoking rate continues to fall steadily. 2019. https://mp.weixin.qq.com/s/6yNn-qHIDx9baXIy0Achpw.[2020-05-18]. (In Chinese).
11. Wu CX. Dispute over amendment of Hangzhou tobacco control legislation. 2018. https://baijiahao.baidu.com/s?id=1603921745444983200&wfrspider&forpc. [2020-05-09]. (In Chinese).

The inauguration of *China CDC Weekly* is in part supported by Project for Enhancing International Impact of China STM Journals Category D (PIIJ2-D-04-(2018)) of China Association for Science and Technology (CAST).

CCDC weekly

Vol. 2 No. 23 Jun. 5, 2020

Responsible Authority

National Health Commission of the People's Republic of China

Sponsor

Chinese Center for Disease Control and Prevention

Editing and Publishing

China CDC Weekly Editorial Office
No.155 Changbai Road, Changping District, Beijing, China
Tel: 86-10-63150501, 63150701
Email: ccdcwjournal@163.com

CSSN

ISSN 2096-7071
CN 10-1629/R1